ADDIS ABABA UNIVERSITY

Addis Ababa Institute of Technology (AAiT)

School of Mechanical & Industrial Engineering (SMIE)

Mechanical Design

A Master's Thesis

Investigation on the Intralaminar Fracture Toughness of Acacia Tortilis/Glass Fiber Reinforced Hybrid Polyester Composite.

A Master's Thesis Submitted to School of Mechanical and Industrial Engineering, Addis Ababa Institute of Technology, Addis Ababa University in Partial Fulfillment of Masters of Science in Mechanical Design.

By: Yohannes Molla

ID: GSR/7154/15

Advisor: Dr. Mulugeta H.

October,2024 G.C

Addis Ababa, Ethiopia

Addis Ababa University

Addis Ababa Institute of Technology

School of Mechanical and Industrial Engineering

Approval of M.Sc. Thesis

Yohannes Molla

Student's name Date Signature

Dr. Mulugeta Habtemariam (Ph.D.)

Advisor Date Signature

Mr.Tolossa Deberie

Internal Examiner Date Signature

Dr. Mesfin Gizaw (Ph.D)

External Examiner Date Signature

Dr. Araya Abera (Ph.D.)

Dean, School of Mechanical Date Signature

And Industrial Engineering

Dr. Sosina Mengistu (Ph.D.)

Associate Director of Date Signature

Postgraduate Program

Declaration

I declared that, the thesis entitled “investigation on the intralaminar fracture toughness of acacia tortilis/glass fiber reinforced hybrid polyester composite” is my own original work, except where properly cited and acknowledged. And it has not been submitted or presented for any degree program in any institution.

Yohannes Molla

Student’s name Date Signature

This thesis work has been submitted for examination with my approval as an advisor.

Mulugeta Habtemariam (Ph.D.)

Advisor Date Signature

Acknowledgment

First and foremost, I thank almighty God for giving me the strength, health, and opportunities as well as chances and making all things possible and succeed.

I would like to express my deepest gratitude to my advisor Dr. Mulugeta Habtemariam who gave me useful and concrete comments, directions, suggestions, and constructive feedback as well as guiding and supervising each step of my work starting from proposal preparation to the accomplishment of the thesis.

I am also deeply grateful to thank Mr. Behailu Mamo for his valuable comments and indicate the possible direction of the work during the proposal defense. I am highly grateful to the Addis Ababa Institute of Technology workshop manager Dr. Hairedin Ismael for his support and cooperation during my stay in the workshop for preparing the composite specimens. I would like to thank Mr. Anteneh Tadiyos, Mr. Esrael Abera, and Mr. Masresha Wondimu for their technical assistance, cooperation, and support during my stay in the workshop.

I would like to express my special thanks to Mr. Biruk Hussien for his unreserved technical and all-round support, cooperation, and friendship throughout my work.

Lastly but not least, I would like to express my thanks to Mr. Yemanebirhan Emiru, a member of the Addis Ababa Science And Technology University Mechanical Engineering workshop for his support during the experimental testing path of my work, and to my family and classmates for their valuable shared ideas and motivations.

Abstract

Natural fiber-reinforced polymer composites as well as their hybridization with synthetic fibers become a choice for their advantages such as being cheap in cost and light in weight. However, the use of these composites for different applications needs an investigation of the fracture behavior of the composite to know the damage tolerance and capability of crack resistance. To study the intralaminar fracture toughness of chopped acacia tortilis/glass fiber reinforced composite, Mode-I intralaminar fracture toughness experimental test on five 2TCT (doubly tapered compact tension) specimens from the four fabricated composite laminates (pure AT (acacia tortilis), pure Glass, and two hybrids H1(G-AT-G-AT-G-AT-G), H2(G-G-AT-AT-AT-G-G)) as per ASTM E399-09 testing standard were carried out. The total fiber volume fraction of the composite laminates was 30% the volume fraction for both hybrid composites was composed of 13% AT fiber and 17% of glass fiber. A recommended data reduction technique based on finite element analysis was employed. From the experimental result, a load-displacement curve for all composite laminates was obtained. The fracture toughness values based on critical energy release rate (G_{IC}) value were evaluated for all composite laminates. The resistance curve (R-curve) was plotted and discussed for all composite laminates. The fractography of fractured surfaces for all composite laminates was qualitatively discussed and from the results, a brittle fracture behavior was observed. The critical energy release (G_{IC}) value for pure AT, Hybrid 1 (H1), Hybrid 2 (H2), and pure Glass composite laminates were evaluated as $1.83\ kJ/m^2$,$24.82\ kJ/m^2$, $21.6\ kJ/m^2$, *and* $37.1\ kJ/m^2$ *respectively. From the result of critical energy release (G_{IC}) values of the four composite laminates, pure AT composite laminate have very small value and hybridization of it with glass fiber resulted a significant change in the G_{IC} value. The two hybrids composite laminates have a G_{IC} value in between the two monolithic laminate composites also have a comparable value with other natural fiber hybrid composites. Finally, a recommendation of the hybrid composite for semi structural or non-structural application was made.*

Key Words: Intralaminar fracture toughness, Acacia Tortilis (AT) fiber, Fractography, 2TCT (doubly tapered compact tension) specimen, R-curve, Critical energy release rate (G_{IC})

Table of Contents

Contents

List of Tables

List of Figures

List of Abbreviations

AT……..…… Acacia Tortilis

CT…….. Compact Tension

2TCT…….....……... Doubly Tapered Compact Tension

VCCT…….Virtual Crack Closure Technique

FRC…… Fiber Reinforced Composite

LEFM……... Linear Elastic Fracture Mechanics

SF……... Synthetic Fiber

NF…….. Natural Fiber

ASTM…… American Society for Testing and Materials

SEM……... Scanning Electron Microscopy

FEA……...Finite Element Analysis

SENB……... Single-Edge Notched Bend

UTM……... Universal Testing Machine

WCT……... Widened Compact Tension

TCT ……... Tapered Compact Tension

ECT ……... Extended Compact Tension

Nomenclature

G_{IC}……... Critical Energy Release Rate

V_f……... Fiber Volume Fraction

E_1……...Longitudinal Young's Modulus

E_2……...Transverse Young's Modulus

V_{12}……...Major Poisons Ratio

G_{12}……...In-Plane Shear Modulus

G_{13}……...Out-Plane Shear Modulus of for 1-3 Plane

G_{23}……... Out-Plane Shear Modulus of for 2-3 Plane

J ……... J-Integral

P_C……...Experimental Load

SD……...Standard Deviation

K_{IC}……...Critical Stress Intensity Factor

1. Introduction

1.1. Background

Nowadays, The widespread use of Natural Fiber Reinforced Polymer Composites in diverse applications is due to their lightweight nature and impressive strength/stiffness characteristics even though they have a hydrophilic nature [1]. FRC is composed of two main components: fibers and a matrix. These fibers can be synthetic or man-made, including those derived from natural resources such as plants. While synthetic fiber-reinforced composites exhibit remarkable mechanical properties compared to their natural fiber counterparts, the drawbacks of synthetic fibers includes non-biodegradability, challenges related to disposal, recycling, and environmental impact [2].

A hybrid composite is the combination of two or more distinct types of fibers within a common matrix. The hybridization of short fibers, characterized by varying lengths and diameters, provides certain benefits compared to using either fiber independently within a single polymer matrix. Many studies have focused on hybridizing natural fibers with glass fibers to enhance properties [3] [4]. The hybridization of natural fibers with synthetic fibers enhances performance and reduces drawbacks associated with both natural and synthetic fibers, enhancing the advantages of both materials [3].

Hybrid composite materials encounter various challenges, including issues like inter-ply cracking, voids, discontinuities, and fiber cracking. Among these concerns, mode I fracture toughness is a prevalent failure mode in hybrid composite materials. The fracture mechanism is very complicated and numerous factors can impact the failure process [5].

Due to various advantages of hybrid composite materials such as light weight, cost effectiveness, and renewability for different applications, in recent times, researchers have focused extensively on investigating the fracture toughness of hybrid composite materials. These increased attentions reflect a growing interest in understanding and improving the performance of these materials in various applications. In this study the intralaminar fracture toughness of Acacia Tortilis/Glass fibers reinforced hybrid polymer composite were investigated using a doubly tapered compact tension specimens (2TCT) as per ASTM E399-09 standard.

1.2. Statement of Problem

These days, Natural fiber reinforced hybrid composite materials have a wide range of applications in engineering due to their renewable, cost-effective, lightweight, and environmentally friendly attributes in contrast to synthetic composite materials, acacia tortilis fiber-reinforced composite is one of the recently introduced natural fiber reinforced composite (NFC) that could be used in many engineering applications. Also from previous literature, its hybridization with glass fiber can be used as a potential composite material for structural and semi-structural applications.

However, the inadequate information and knowledge of their fracture toughness properties is one of the reasons for their limited practical use in structural or semi-structural applications. Adequate knowledge of their fracture toughness behavior plays a significant role in the various practical engineering applications, specifically in designing for damage tolerance and assessing residual strength and structural integrity. This helps to increase the lifetime of the composite material by decreasing catastrophic failure. As far as my review of different literature, there is no available data about the intralaminar fracture toughness characterization of acacia tortilis fiber-reinforced composite. Therefore, this study addressed the stated problem by investigating the intralaminar fracture toughness of acacia tortilis/glass fiber reinforced hybrid polyester composite experimentally under Mode I loading conditions.

1.3. Objectives of the study

1.3.1. General Objectives

The main objective of this research is to investigate the intralaminar fracture toughness of Acacia Tortilis/Glass fiber reinforced hybrid polyester composite experimentally under Mode-I loading conditions.

1.3.2. Specific Objectives

The specific objectives of this study include:

- Determining the polynomial coefficients using FEA (Abaqus/CAE 2016).
- Analyzing load-displacement curves from the experimental test.
- Determining the critical energy release rate (G_{IC}) values.
- Analyzing the crack growth resistance curves ($G_{IC}\ Vs\ a$) of the composites.

- To qualitatively discuss fractography of a fractured surfaces using a digital camera.

1.4. Delimitation of the Study

The study focused on the experimental investigation of the intralaminar fracture toughness of Acacia Tortilis/Glass fiber reinforced polyester composite. So, the evaluation of fracture toughness based on the critical energy release rate, analysis of a resistance curve, and a qualitative discussion of fractography for a fractured surface of the composite laminates has been focused. Whereas the effect of the plant's geographical location, aging of the plant, condition of the plant while extracting (live or dead), and extraction technique of the fiber, the effect of fiber collected from different climatic conditions were not focused. Moreover, the effect of water absorption on the fracture toughness of the composite was not covered.

1.5. Significance of the Study

By determining the intralaminar fracture behaviors of acacia tortilis/glass fiber reinforced hybrid composite, the study plays a significant role in positioning the composite as a viable alternative to non-biodegradable synthetic fiber composites, providing crucial insights into its damage tolerance, crack resistance, and fracture toughness, which are essential for preventing catastrophic failure and ensuring the reliability, safety, and optimal performance of structures and components in various engineering applications, thereby enhancing its design for lightweight, cost-effective applications in structural, semi-structural, or non-structural contexts, while also contributing to materials science and quality assurance processes and serving as an input for further research and development in engineering.

1.6. Organization of the study

This work is structured into five chapters. The first chapter includes introduction and background description on natural fiber composite materials, synthetic fiber composite materials, and hybrid composite materials. the general and specific objectives, statement of the problem, delimitation and significance of the thesis. The second chapter presents a comprehensive literature review on the different topics that are relevant to the study. The third chapter presents the materials and methods, the experimental setups and procedures. The fourth chapter deals with experimental results along with finite element (FEA) computational result, analysis and interpretation of these results. The last and fifth chapter provided conclusions, recommendations and suggestion on future work.

2. Literatures Review

2.1. Introduction

In this section a review on different topics of the composite material, on acacia tortilis/glass fiber reinforced composite, on fracture behaviors, and on testing standards has been done. Furthermore, a review of some of the previous works that are related to this study was incorporated.

2.2. Composite Material

Composite material is a material that consists of two or more materials that are combined at a macroscopic level with different physical, chemical properties, and mechanical properties. but the individual components remain separate, not soluble in each other, and distinct in the final product [6], [7].

The distinct characteristics of these composites arise from the unique properties of their individual components, along with their respective volume fractions and arrangements within the material. The utilization of composite materials has resulted in decreased costs, enhanced efficiency, and improved utilization of existing resources. Designed for specific purposes, composites can be engineered to meet precise geometric, structural, mechanical, chemical, and sometimes aesthetic criteria, depending on the intended application. Composite material has wide applications in industries such as aerospace, automotive, and manufacturing [8], [9].

The material, which is embedded in it, is called reinforcement and the material in which it is embedded is called the matrix. The reinforcement phase commonly existed in the form of fibers or flakes/chopped but sometimes it existed as particles. Composite has a reinforcement phase that is stiffer and stronger than the continuous matrix phase which serves as the principal load carrying members. The nature and properties of the reinforcement materials and matrix used as criteria for the classification of composite materials [6], [7].

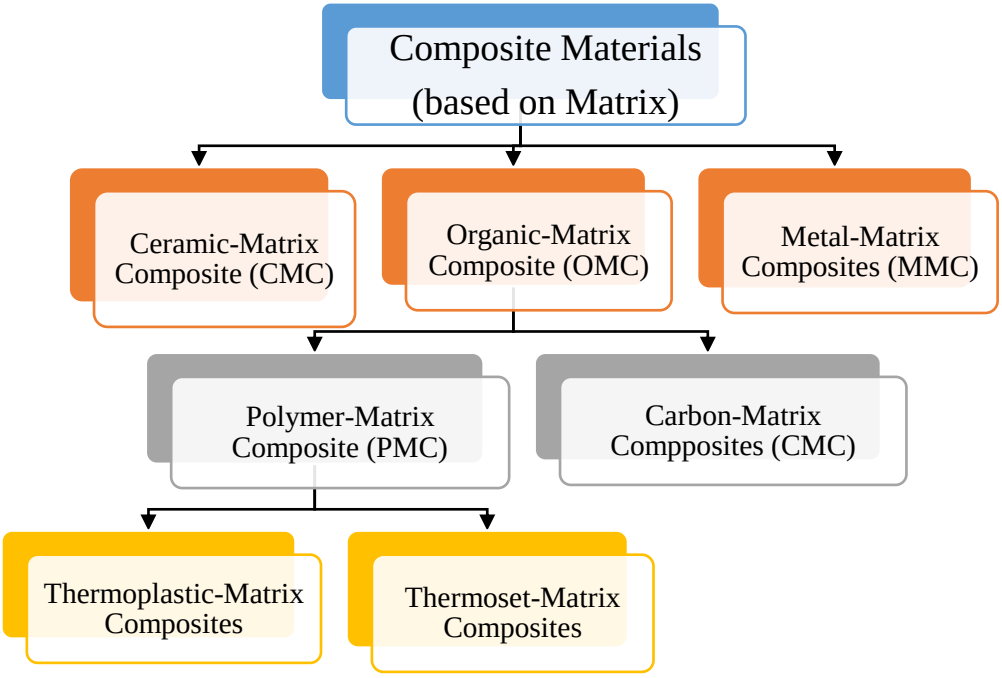

Figure 1 classification of composite materials base on matrix materials *[10]*

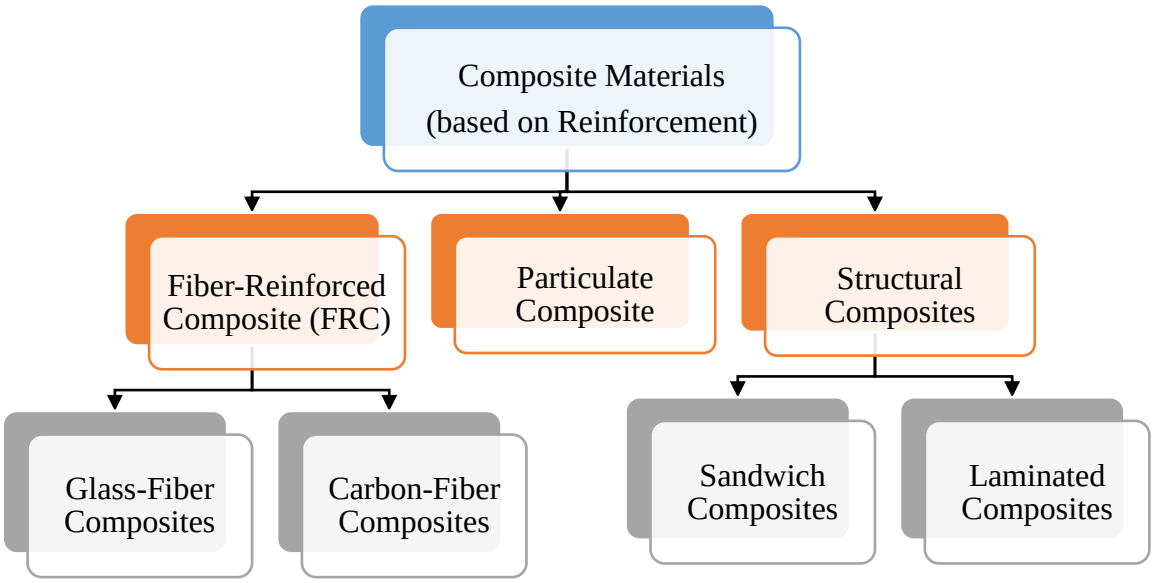

Figure 2 classification of composite materials based on reinforcement materials [10]

2.2.1. Laminated Composite Material

The properties of composite materials are influenced by the quantity of matrices and reinforcements, as well as the manufacturing techniques employed. A laminate is formed by bonding individual plies together to their principal plane [11], [12]. Composite laminates are formed by layering different plies at various angles and orientations [13].

The composite material, reinforced with fibers, is made by combining fibers within a thin layer of the matrix to generate a lamina (ply). The lamina is constructed using continuous and discontinuous fibers, arranged in either a unidirectional, bidirectional, or multi-directional orientation [14], [1].

When designing a laminate, it is crucial to take into account the arrangement of plies, ensuring symmetry and balance in the stack. An asymmetrical stack is effective in reducing bending or warping tendencies [15].

Multiple laminas are stacked and joined in the specified alignment to create a laminate, achieving the necessary thickness to sustain a specified deflection or support a particular load in a fiber-reinforced composite [12]. The typical thickness for laminas usually falls within the range of 0.1mm to 1mm [1].

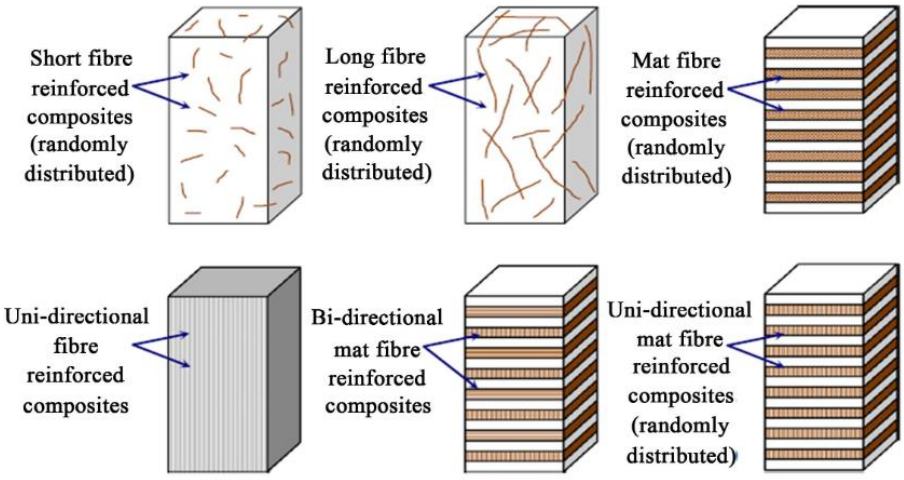

Figure 3 different type of fiber orientation used for laminate manufacturing *[16]*

2.3.Synthetic Fibers

Synthetic fibers/artificial fibers/ are employed for reinforcement purposes, including carbon, glass, and aramid fibers. Glass fibers, in particular, are widely employed due to their abundance and cost-effectiveness. Common forms of glass fiber reinforcement include continuous fibers, used in processes like weaving, winding, and braiding, as well as discontinuous fibers, which are formed by cutting continuous fibers. Woven fabrics, designed for laminates, have applications in various fields such as boating, sports, marine activities, and applications using multidirectional fabrics [1].

SF (Synthetic fibers), known for their high strength and resistance to chemical reactions, are extensively utilized in the aerospace and automotive industries for fabricating advanced composite materials. The superior flexibility, elasticity, water resistance, chemical resistance, and heat resistance of SFs make them better than and overtake NFs (Natural Fibers). SFs address the shortage of NFs, as the supply of NFs is insufficient for industries such as aerospace, defense, automotive, wind energy, and pipe manufacturing that exhibit significant demand for composites based on glass, carbon, and aramid fibers [17].

Synthetic glass fiber composites face challenges in terms of recycling, reusability, and biodegradability issues upon reaching the end of their useful life. Therefore, a viable solution involves combining natural fibers with synthetic fibers to enhance the strengths of both types of fibers. This approach allows the advantageous properties of each fiber to counterbalance and compensate for the shortcomings of the other.

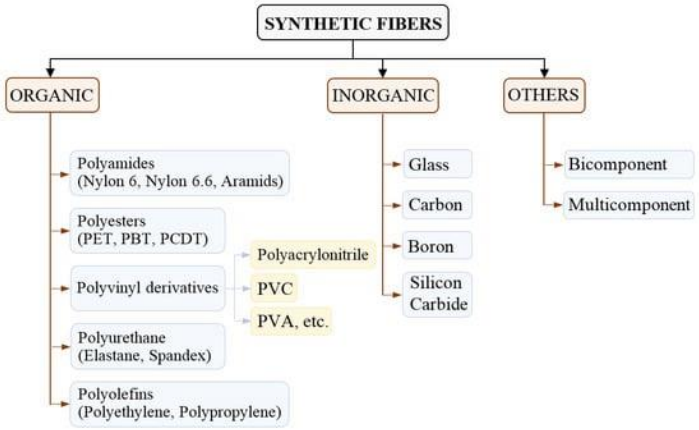

Figure 4 classification of synthetic fibers*[17]*

2.3.1. Glass Fiber

Synthetic fibers are categorized into organic and inorganic varieties. Among the inorganic fibers, glass fibers, commonly known as fiberglass, serve as reinforcements in composite materials. Glass fibers offer notable advantages, including high strength, cost-effectiveness, superior chemical resistance, and low density. There are different classifications of glass fibers which are: C-glass is utilized to reinforce corrosive limitations in chemical plants, enhancing surface finish. D-glass is employed for applications with low strength requirements, while E-glass is employed in applications that need beautification, structural, and electrical uses. S-glass, characterized by a high silica content and strong fatigue resistance, is preferred in aerospace applications. Unlike Kevlar or Carbon fiber, Glass fibers exhibit isotropic properties, ensuring the sustainability of strength when loaded in the transverse direction [1], [18].

2.4. Natural Fibers

Natural fiber composites (NFCs) are a possible alternative to traditional synthetic fiber materials such as fiberglass. Natural fibers such as acacia tortilis, sisal, abaca, bamboo, banana, coir, flax, hemp, jute, kenaf, pineapple leaf, and others, are advantageous due to their reduced weight, cost-effectiveness, non-toxic, less susceptible to health hazards, recyclable, renewable, competitive mechanical properties, impressive specific strength, and potential for biodegradability. NFCs have practical and environmentally friendly options to conventional composite fibers in sectors like construction, automotive, and packaging [19], [20].

The mechanical and moisture absorption characteristics of composites containing natural fibers are notably impacted by the interfacial bonding between the fiber and the matrix. To enhance this bonding, an improved adhesion is required by treating the fiber surfaces with alkaline solutions [21].

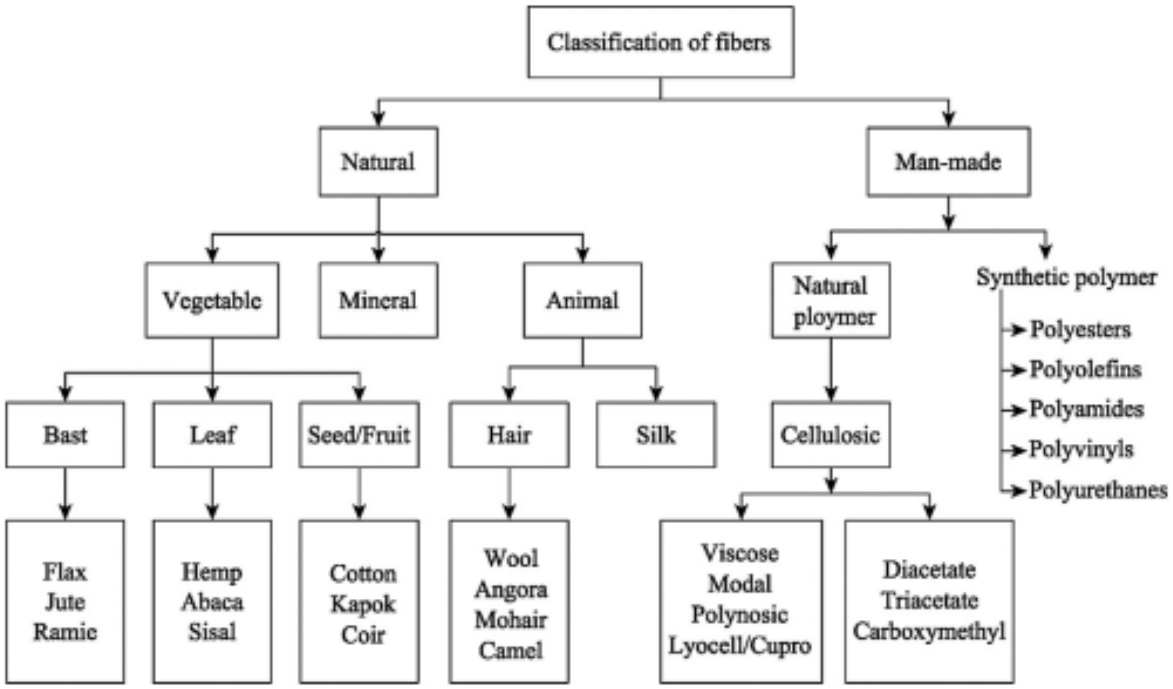

Figure 5 classification of fibers *[22]*

Acacia Tortilis natural fiber is categorized in the Bast/Skin part of the vegetable natural fiber classification.

2.4.1. Acacia Tortilis Plant

Acacia tortilis, a drought-resistant plant from the Fabaceae family, thrives in arid and semi-arid regions of North Africa, the Arabian Peninsula, and other harsh environments, playing a key role in local ecosystems and benefiting humans, animals, and plants. [23], [24].

The Acacia Tortilis plant is utilized to fix nitrogen and helps in reforestation efforts. It plays a crucial role in improving soil fertility and facilitating the establishment of new forests [24], [25], [26].

Figure 6 Acacia Tortilis Tree

2.4.2. Acacia Tortilis Plant in Ethiopia

Acacia Tortilis (Figure 6), commonly referred to as Girar in Ethiopia, constitutes significant vegetation in the arid and semi-arid regions of the country. It is known for its drought-resistant qualities; this species grows in areas with annual rainfall ranging from 40 mm to 1200 mm and can endure temperature fluctuations between 0°C and 50°C. Beyond its adaptability, the Acacia Tortilis plant serves various purposes, including providing fuelwood, Feed, and shelter. Additionally, it has the potential to enhance soil fertility, contributing to increased crop productivity in Ethiopia's arid and semi-arid zones [6], [23].

In Ethiopia's rural regions, these plants act as primary suppliers of firewood and charcoal. Moreover, they have the ability to improve soil fertility, leading to increased crop productivity [27].

Studies have investigated the Acacia Tortilis plant, examining its uses for fuelwood, feed, and shelter, enhancement of soil fertility, nitrogen fixation, and reforestation. Additionally, its significance for pharmaceutical and biological applications has been explored [28], [29], [30], [31]. Moreover, its potential application as a green fiber source for strengthening composite structures has also been explored [32].

2.4.3. Acacia Tortilis Fiber

Acacia Tortilis fiber naturally exists as a twisted or spun-together fiber unlike other common natural fibers, and it is found in the stem skin/bark of the tree simply smooth part of the bark is the fiber itself. The chemical composition of acacia/tortilis fiber is summarized in the following table.

Table 1 chemical composition of Acacia/Tortilis fiber [32]

cellulose	Lignin	Wax	Moisture content	Ash content	Density
61.89%	21.26%	17.43%	6.47%	4.33%	0.906g/cm^3

2.5.Mechanical Properties of Acacia Tortilis Fiber

Dawit et al. [32] studied the property characterization of acacia tortilis fiber and from the result of the study the tensile strength, tensile modulus, and elongation(%) is 71.63 MPa, 4.209, 1.33 respectively.

2.6. Mechanical Properties of Acacia Tortilis/Polyester Composite

Even though studies on the characterization of mechanical properties of acacia tortilis fiber-reinforced polymer composite are very limited and the fiber itself was introduced a few years ago, The tensile strength of acacia tortilis polymer composite is 20.14 MPa, and the flexural strength of 77.5 MPa [20].

2.7.Composite Fabrication Methods

In the process of fiber-reinforced composite fabrication, first, the fiber is processed and ready for reinforcing and then it is reinforced with the matrix material using different methods of composite fabrication. Some of the conventional composite fabrication processes are hand lay-up, vacuum bag molding process, resin transfer molding, compression molding, spray-up, injection molding, pultrusion process, and filament winding techniques. [33] Reviewed thus and other conventional as well as automated fabrication methods of fiber-reinforced composites (FRCs). From those hand lay-up is the most basic, easy, and widely used method of composite fabrication.

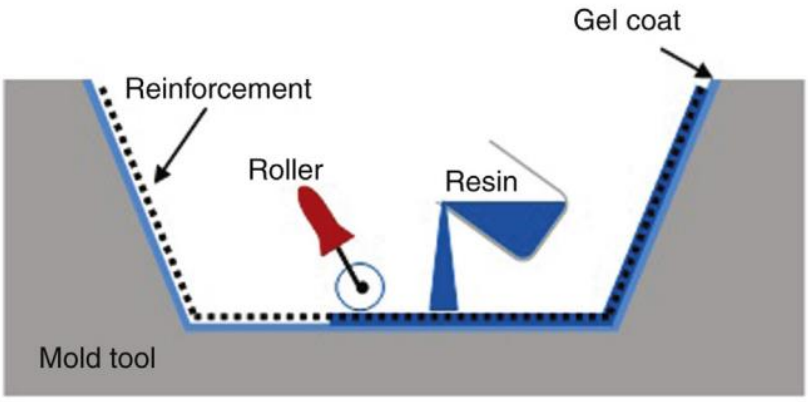

Figure 7 hand lay-up method [34]

2.8. Alkaline (NaOH) Treatment of Acacia Tortilis Fiber

Acacia tortilis has a chemical composition of 61.89% cellulose, 21.26% lignin, 17.43% Wax and 4.33% Ash [32]. The percentage contents of the fiber other than the cellulose leads to lowering the mechanical properties and leads to unwanted water absorption properties. The Chemical treatment of natural fibers is used to remove waxy substances, lignin, and natural oils from the surface of the fiber cell wall and removal of these waxy substances enhances the adhesion properties for the fiber-matrix interface, roughness of the fiber, fiber shear strength. The common chemical treatment of natural fibers includes alkaline treatment and alkali-silane treatment. and other chemical treatment types used for the refinement of natural fibers are Acetylation, Benzoylation, peroxide, and Esterification [35]. Alkali treatment is one of the common fiber treatment methods and it is used to increase strain at break [36], and it is the most effective fiber treatment for cleaning the fiber, both the fiber components and impurities [37].

In the previous study, Dawit et al. [32] performed alkaline treatment on acacia tortilis fiber with 10% and 20% alkaline concentrations. The AT fiber treated with 10% concentration showed improvements in mechanical properties compared to 20% concentration treatment & untreated acacia tortilis fiber.

2.9. Hybridization of Natural fibers and synthetic fibers

Hybrid composite are materials that consists of various synthetic or natural fibers systematically combined within a single polymer matrix to attain a desired properties where the undesired properties/disadvantage/ of one fiber can be compensated with the second fiber [38], [39].

Natural fiber reinforced polymer hybrid composite can be classified into three types, depending on how reinforcements are distributed. These are interplay, intraply, and super hybridization. Interplay occurs when different constituents are layered within the laminate. Intraply hybridization involves parallel combinations of constituents within individual plies. Super hybridization includes layers where metal/composite and matrix are arranged in a specific sequence [39].

Hybridizing synthetic fibers with natural fibers is an effective method employed to enhance mechanical properties, including increased strength and stiffness, thermal stabilization, and improved resistance to fatigue and moisture. This approach surpasses the mechanical properties of natural fibers alone[14]. It is important to attain a balanced mechanical and thermal property as well as enhance the durability of natural fiber composites [38], [39], [40]. Hybridizing materials to enhance their properties has consistently been a promising strategy for producing a new and innovative material [40].

2.9.1. Mechanical Properties of AT/Glass Fiber Hybrid Composite

Dawit et al. [6] studied the mechanical properties (flexural and tensile) of acacia tortilis/ glass fiber reinforced hybrid composite. The glass fiber was randomly oriented and the acacia tortilis fiber was treated and chopped. Following the conventional hand lay-up method and total fiber wt% of 40 (20/20: AT/GF) fabricated the composite and prepared the specimens for tensile and flexural as per ASTM standards D3039 and D7264-07 respectively. The test result indicates that tensile strength of 61.12 MPa, Flexural strength of 249 MPa, and 4.06 MPa of Young's modulus.

The addition of glass fiber to the acacia tortilis fiber has shown improvements in mechanical properties compared to the pure acacia tortilis polymer composite studied previously by the same researcher [20].

2.10. Matrix Materials

The matrix serves as a crucial component and a continuous phase within the composite. Its function is to unite and transfer mechanical loads through the fibers to the overall structure. Additionally, the matrix plays a role in binding the fibers together. Moreover, it provides a protection for the fiber against environmental factors such as abrasion, impact, humidity, and corrosion [14].

The Composite material will be fabricated by reinforcing the fibers with hydrophobic (water repelling) thermoset matrices.

Thermoset matrices such as polyester resins have advantages in exhibiting dimensional stability, rigidity, electrical and thermal insulation properties. Varieties of thermoset matrices include viscous liquid and powdered resin.

Polyester resin has wide applications in diverse structural and non-structural application sectors such as construction, aircraft manufacturing, automotive, marine, packaging, furnishings, and textiles. They have the capability to take on the desired shape, whether applied wet or dry, and they exhibit rapid drying. Additionally, polyester resins resist stretching and wrinkling/folding, and they offer durability against shrinking, and abrasion, while maintaining a colorless and transparent quality[18]. for these benefits of the polyester resin and it is compatible with acacia tortilis fiber [32] and with glass fiber[41], it was used as a matrix material for this study.

2.11. Fracture Mechanics

Fracture toughness serves as an indicator of the stress required for the propagation of an existing crack, and it has immense significance as cracks are unavoidable during the processing, fabrication, or service of a material/component. Defects can occur in various forms like cracks, voids, metallurgical inclusions, weld defects, design discontinuities, or a combination of them.

Since absolute certainty about the absence of cracks in a material is unattainable, engineers commonly assume the presence of a crack of a chosen size in some components. The linear elastic fracture mechanics (LEFM) approach is then employed to design critical components, considering factors such as crack size, features, component geometry, loading conditions, and the material property known as fracture toughness. In this approach, the stress intensity factor (K) is a crucial parameter used to predict the stress state near the tip of a crack caused by varying load or residual stresses [42].

2.11.1. Failure Modes of FRCs

The failure mechanisms of FRCs depending on the remotely applied stress to unidirectional composite consists of fiber breakage (in tension), fiber micro buckling and kinking (in compression) and it is due to fiber misalignment, matrix cracking (brittle or ductile), and fiber/matrix debonding. Matrix failure in composite material can be classified in to two types:

intra-ply failure, where there is fracture between fibers within a single layer (known as inter-fiber fracture), and inter-ply failure, specifically delamination. Intra-ply matrix failure typically initiates at the fiber-matrix interface and speeds into the matrix itself. Whereas delamination occurs due to micro-cracks forming in the matrix between different layers, which is a consequence of significant stresses between the layers [43], [44], [45].

2.11.2. Modes and types of Fracture

The final failure of laminated composite structures is preceded by various damage mechanisms involving fracture initiation and propagation. Assessing when fracture begins, how fracture propagates, and understanding associated fracture toughness are crucial factors in designing efficient and durable fiber-reinforced composite structures. Fractures in composite laminates can occur either between two plies (interlaminar fracture or delamination) or within a single layer (intralaminar fracture). In interlaminar fracture, cracks cause separation between adjacent layers of the laminate. The crack propagation primarily involves failure of the matrix or debonding between the matrix and fibers. Although some fiber failures bridging of the delamination may also occur. In the intralaminar or translaminar fracture, which is typically identified by a crack that propagates parallel to the fibers across the thickness of the layers, it is essential for analyzing transverse matrix cracking. The crack occurs within the lamina itself and can be oriented either parallel to the fibers (resulting in matrix cracking) or at an angle (involving fiber failure). When an intralaminar crack propagates at an angle to the reinforcing fibers, these fibers bridge both surfaces of the crack, halting or minimizing further opening of the crack until these bridging fibers break. even if the energy consumed in fiber fracture is usually much larger than in matrix cracking or fiber-matrix debonding [46] [47].

As shown below, Interlaminar crack/delamination/ is defined as a discontinuity in the x-y plane between two adjacent plies of a laminate. Whereas Intralaminar crack is defined as a discontinuity in the y-z plane, which advances through the entire laminate thickness in the direction parallel to the fiber direction [48].

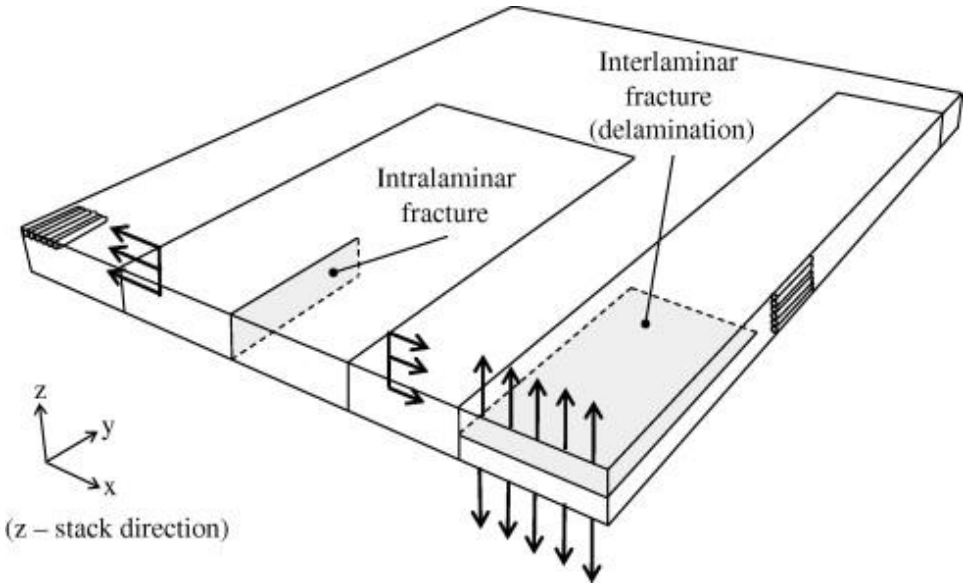

Figure 8 difference between intralaminar and interlaminar fracture of Mode I fracture.*[48]*

Modes of fracture are determined by how a crack propagates through a material. These modes are mode I, mode II, mixed mode (mode III). The figure below shows the different modes of crack. Mode I is characterized by crack opening or delamination caused by tensile load. Mode II is characterized by an in-plane shear mode of delamination. Mode III is characterized by tearing or out-of-plane shear. Typically, the fracture mechanics study of metal focuses primarily on mode I [49], [50].

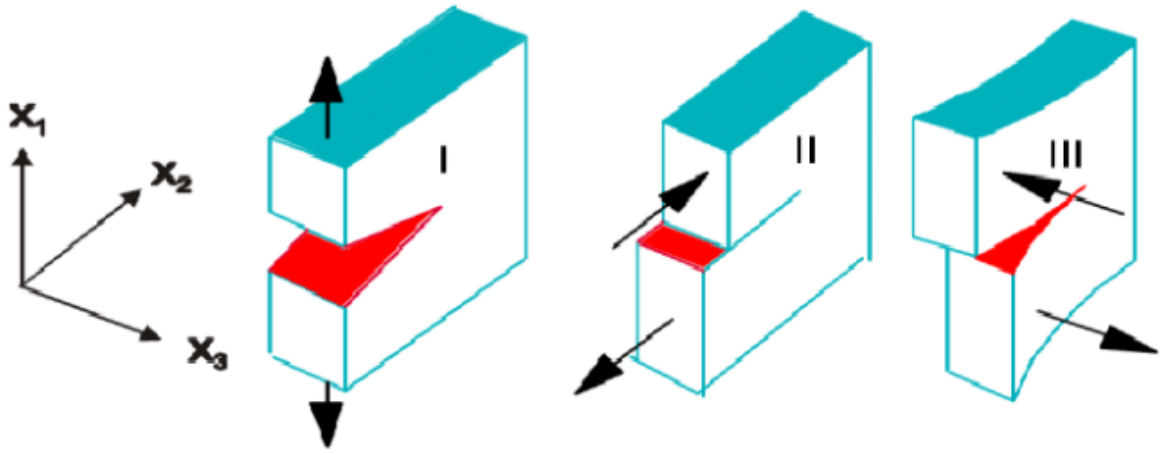

Mode I (Opening mode) Mode II (Sliding mode) Mode III (Tearing mode)

Figure 9 the three basic crack modes *[51]*

2.11.3. Common Fracture Toughness Test Standards

There are different commonly used ASTM standards used for testing fracture toughness parameters of fiber reinforced composite (FRC) materials. In ASTM E399-09 standard, the compact tension specimen (CTs) is initially developed for determining the crack propagation of metallic materials and used to determine the fracture toughness (K_{IC}) of metallic materials predominantly under linear-elastic, plain-strain conditions using fatigue pre-cracked specimens [52]. It has also been commonly used for testing and determining the intralaminar fracture toughness of fiber reinforced polymer composite (FRPC) materials.

In the ASTM D5045-14 standard, the compact tension specimen (CTs) is initially developed to determine the intralaminar fracture toughness of plastic materials [53]. It has also been commonly used for testing and determining the intralaminar fracture toughness of fiber-reinforced polymer composite (FRPC) materials.

The other ASTM standard specimen for measuring fracture toughness in laminated composite is the Extended Compact Tension (ECT) specimen (E1922-04) [54]. Initially developed for testing the fracture properties of ceramic materials, this specimen is a modified version of the compact tension (CT) specimen, with an increased height. The current ECT specimen is now used to investigate fatigue crack growth and fracture behavior in metallic materials. This design helps to reduce stress parallel to the crack surface [55].

The other specimens are the widened compact tension (WCT), the tapered compact tension (TCT), and doubly tapered compact tension (2TCT), the widened compact tension (WCT) developed for reducing the compressive stresses induced in this area of the specimen which might cause failure due to vertical compressive fiber breaking. With the same purpose of reducing the compressive stress generated, a tapered compact tension (TCT) specimen was designed in a variation of the CT specimen in which the right edge of the specimen had been tapered [55].

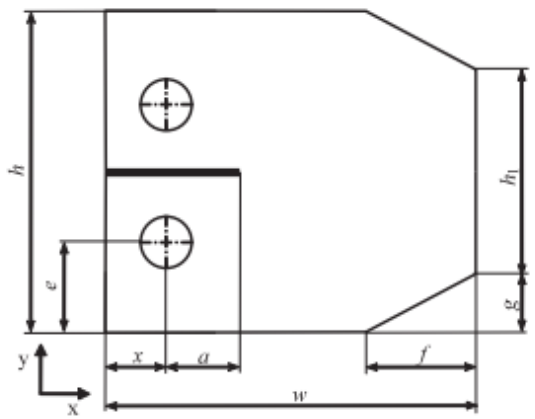

Figure 10 CT, ECT, WCT, and TCT specimens with geometric parameters[55]

To ensure the crack propagation for experimental characterization will occur without interference from other damage mechanisms, Blanco et al.[55] studied the intralaminar fracture toughness characterization of woven composite laminates (design and analysis of a compact tension (CT) specimen), various geometric designs/configurations of the compact tension (CT) specimen were investigated for the characterization of the tensile intralaminar fracture toughness of woven composite laminates. The study conducted parametric finite element (FE) analyses, along with virtual crack closure technique (VCCT) methods for these different geometries. Based on the studies, the doubly-tapered compact tension (2TCT) specimen was chosen as the most suitable and appropriate specimen geometry. The 2TCT specimen geometry proposed by this researcher is shown below where the thickness is 5.6 mm and the initial crack size is 20mm.

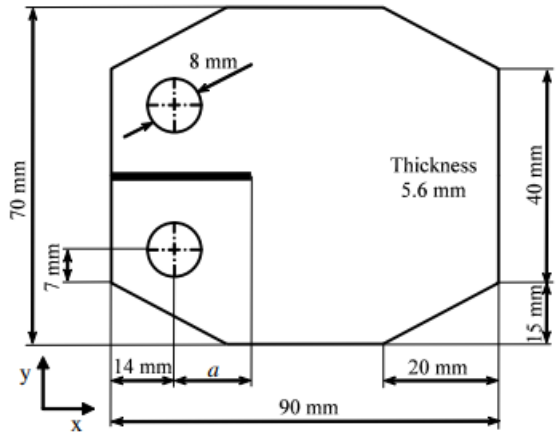

Figure 11 the proposed doubly tapered compact tension (2TCT) specimen[55]

2.12. Review of Some Related Previous Work

As previous researchers[32] studied on experimental characterization of Acacia Tortilis fiber for natural fiber-reinforced composite material, the paper finds out that acacia tortilis fiber is an alternative source of natural fiber for NFC material. Also, the same researcher [6] studied on hybridization of AT fiber with glass fiber to investigate the mechanical properties specifically the tensile and flexural properties, and the study found promising results.

From previously related literature that studied acacia tortilis fiber and from works on fracture toughness of different composite materials some of them are here below.

Dawit et al**.** [32] Performed a characterization study of the properties of acacia tortilis for a natural fiber-reinforced polymer composite, acacia tortilis was obtained and investigated as a natural fiber for use in green composites according to the ASTM standard for sample preparation and experimental testing of fiber bundles. The extracted fiber was subjected to an examination of chemical composition, density, and tensile strength. In addition, the effect of chemical treatment on fiber bundles was investigated and promising results were obtained. They concluded that Acacia Tortilis fiber has potential as a natural fiber for green composite applications compared to published findings.

By the same researcher [20] the mechanical properties of Acacia tortilis fiber-reinforced natural composite have been investigated Experimentally. They investigate the mechanical properties of a new composite material made from Acacia tortilis fiber and reinforced with polyester using experimental techniques. Specifically, the investigation focuses on the evaluation of the tensile and flexural characteristics of the composite at different fibers volume ratios of fabricated using hand lay-up methods. The results revealed that Acacia Tortilis fiber-reinforced polyester composites generally exhibit competitive tensile strength of 71.63 MPa and Young's modulus of 4.209 MPa compared to commonly use natural fiber-reinforced composites such as sisal, kenaf, and coir. In addition, the NaOH-treated samples have higher strength and Young's modulus compared to their untreated counterparts.

By previous researcher [6] the tensile and flexural properties of Acacia Tortilis/glass fiber hybrid composites have been studied. The study fabricated and analyzed a hybrid composite reinforced with Acacia tortilis and glass fiber (AT/GF). After the successful fabrication of the Acacia tortilis/glass fiber (AT/GF) hybrid composite using hand layup techniques, tensile and

flexural tests were performed and yields promising results (tensile strength of 61.12 Mpa and flexural strength of 249 Mpa). By Comparison of these findings with previous reports and published results they suggested that the hybrid Acacia tortilis/glass fiber reinforced composite has potential for a variety of structural and non-structural applications. The authors also recommend further investigation into the various properties of the Acacia tortilis/glass fiber hybrid composite.

Blanco et al. [55] Studied on characterization of the intralaminar fracture toughness of woven composite laminates (compact tensile CT specimen design and analysis). Different geometries of compact tensile (CT) specimens were investigated to characterize the tensile intralaminar fracture toughness in woven composite laminates. The goal of the paper was to ensure that the necessary crack propagation for experimental characterization occurs without interfering with other damage mechanisms. Parametric finite element analyzes in conjunction with the virtual crack closure technique (VCCT) were performed for these different geometries. Based on the analyses, double tapered compact tension (2TCT) was identified as the most suitable geometry for the sample.

By the same researcher [47] the tensile interlaminar fracture toughness of woven carbon/glass composite material 5HS-RTM6 using a doubly-tapered compact tension(2TCT) specimen have been characterized Experimentally. The geometry of this sample showed lower values for the failure indices presented in the first part of the article (PART I). Two material configurations were investigated: one with the direction of material deformation aligned parallel to the applied load and the other with the direction of deformation perpendicular to the applied load. The study found similar values of mode I intralaminar fracture toughness for both configurations. Analysis of DIC images, X-ray, and C-scans concluded that the presence of other damage mechanisms other than Mode I intralaminar crack opening was negligible. Consequently, the obtained experimental values were considered reliable/trustworthy and confirmed the usefulness of the 2TCT sample for its intended purpose.

Pinho et al**.** [45] Studied the fracture toughness of tensile and compressive failure of fibers in a laminated composite. The fracture toughness of T300/913 carbon-epoxy laminated composite was investigated by evaluating the fracture toughness associated with fiber failure in tension and fiber kinking in compression through compact tension and "compact compression" tests. A

digital speckle photogrammetry system was used to monitor the deformation fields in the samples during the tests. After the test, the damage in the samples was examined using C-scan, optical microscopy and scanning electron microscopy (SEM). The critical energy release rate for initiation and propagation of tensile fiber failure was determined to be 91.6 kJ/m^2 and 133 kJ/m^2 respectively. An initiation value of 79.9 kJ/m^2 was obtained for fiber compression kinking, but meaningful propagation values could not be determined. The test results showed low scatter for both cases.

Pinto et al.[56] Studied measuring the intralaminar crack resistance curve of fiber-reinforced composites at extreme temperatures. The primary focus of the study was to develop techniques for assessing the intralaminar fracture toughness of IM7/8552 CFRP (carbon fiber reinforced polymer) under extreme temperatures. To achieve this, the researchers utilized the size effect law of scaled double-edge-notched specimens, which allowed them to derive crack resistance curves related to the longitudinal failure of polymer composites. The crack resistance curves for both compression and tension were determined and compared to those obtained at room temperature. Additionally, scanning electron microscopy was employed to examine the fracture surface of the tensile double-edge-notched specimens, providing insights into the damage mechanisms and their relationship to temperature variations. The findings demonstrated that the proposed methods are effective in measuring the crack resistance curve under diverse environmental conditions. The researchers recommended utilizing the obtained results in analytical models to assess the structural integrity of composite materials used in extreme temperature environments.

Zhao et al. [57] studied the intralaminar crack propagation of glass fiber-reinforced composite laminate. The study aimed to investigate the propagation of cracks within the layers of a unidirectional glass fiber-reinforced polymer composite laminate. The investigation was carried out through quasi-static tensile and compression experiments, supported by finite element analysis (FEA). The experimental results indicated that the intralaminar crack propagation was accompanied by fiber bridging, which was further confirmed through scanning electron microscopy (SEM) observations. Additionally, multiple cracks were observed in specimens without pre-existing cracks. The calculated value of intralaminar fracture toughness in a stable state was approximately 4.5 N/mm. The extended finite element method predictions of the crack distribution within the representative volume element were in agreement with the SEM results,

indicating that crack propagation was associated with matrix cracking, interfacial debonding, fiber pull-out, and fiber fracture. The paper concluded as, a combined approach involving the progressive damage model and extended finite element method with representative volume element showed promise in simulating intralaminar crack propagation, which could help in gaining a deeper understanding of the micro-macro failure mechanism.

Araya Abera et al. [58] investigated the intralaminar fracture toughness of chopped sisal/epoxy composites with fiber weight percentages in the range of 15-40% using the CT method and the ASTM D5045 standard. The composites were developed using hand layup and molding techniques. Fracture toughness tests were performed at a crosshead speed of $0.5mm/min$ using a universal testing machine (UTM). The study found that the value of KIC increased with fiber content and peaked at $K_{IC} = 5.54\, MPam^{\frac{1}{2}}$ ($G_{IC} = 13.72\, kJ/m^2$) at 30% fiber weight percentage and decreased beyond it.

Hughes M. et al. [59] performed a SENB test to compare the intralaminar fracture toughness of chopped hemp and jute fiber-reinforced polyester composites and chopped strand mat glass fiber-reinforced laminate. The K_{IC} of NFC value was three times lower than the volume equivalent (V_f = 0.2) of the glass fiber composite. This is because NFCs do not drive microstructural toughness mechanisms as much as GFRP composites.

Silva et al. [60] used the compact tension (CT) method to investigate the effect of fiber type, architecture, treatment, and displacement rate on the fracture toughness (G_{IC}) of sisal and coir fiber reinforced castor oil polyurethane composites. Short fibers and fabrics were investigated with and without 10% NaOH treatment. The study found that woven sisal fabric had the highest G_{IC}, while short sisal fibers performed better than coconut fiber reinforced composite. Alkaline treatment decreased GIC of sisal fiber/castor oil polyurethane composite. Alkaline treatment increased the fracture toughness of coconut fiber/castor oil polyurethane composite. They also found that strain rate has no significant effect on fracture toughness.

Zhang et al. [61] investigated the effect of interply hybridization on the fracture toughness (G_{IC}) of composites made from synthetic and natural fibers. Unidirectional flax/glass fibers reinforced Phenolic resin was investigated by the DCB method. The hybrid composites outperformed the

pure glass fiber composites in terms of fracture toughness due to better performance at the hybrid interface.

P. S. S. Gouda. [62] Performed experimental and finite element studies on the mode I fracture behavior of glass carbon fiber reinforced hybrid composites using compact tensile (CT) specimens. The study found that cracked specimens are tougher along the fiber orientation rather than across. In addition, the modulus of elasticity of the tensile specimen and the critical stress intensity factor (K_{IC}) of the CT specimen show greater severity along the fiber orientations. The finite element results show that the key stress intensity factor (K_{IC}) dominates along the fiber direction of the CT specimen.

Donadon et al. [63] studied numerical and experimental studies of Mode-I intralaminar fracture toughness in a hybrid plain weave composite laminate fabricated by resin infusion under flexible tooling. Over height compact tension, double edge notched and centrally cracked four-point bending specimens were used. Digital point photogrammetry monitored the crack tip position and strain field during loading. The paper discussed the limitations of standard data reduction methods for determining composite intralaminar fracture toughness and proposed a new methodology, which uses a numerical calculation of the geometry of specific correction functions to determine the stress intensity factor in composites. The paper compares existing methods for calculating composite intralaminar fracture toughness and demonstrates good agreement between experimental results and the proposed methodology.

Naik et al. [64] studied the mode I fracture toughness in terms of stress intensity factor (K_{IC}) for banana fiber-reinforced polymer composite using the LEFM approach, and mechanical properties of composites reinforced with short banana fibers using a compact tensile specimen. The results show that the 40% banana fiber has the highest fracture toughness, while the 30% composite panel has the highest tensile strength. Increasing the fiber content improves the material's fracture toughness and tensile strength.

2.13. Research Gaps

As per different previous studies on different composites, the use of laminated composite for different engineering applications needs an investigation on fracture behavior of the material to increase life time of the material knowing the fracture resistance capability of the material. Fracture toughness characterization of NFC and their hybrids is necessary due to the increasing

use of these materials and the desire for an environmentally friendly, cost-effective, damage-resistant and optimized product. From the different literature it is evident the intralaminar fracture toughness behaviors of acacia tortilis/glass fiber hybrid polymer was not done before. even though the literatures on this typical acacia tortilis (*Girar*) fiber reinforced composite is very few some mechanical properties of acacia tortilis fiber reinforced polymer composite and its hybridization with glass fiber was studied by Dawit et al.[6], [20], [32]. By the case this study will address the gap by investigating the intralaminar fracture toughness of acacia tortilis/glass fiber reinforced hybrid polyester composite with doubly tapered compact tension specimens (2TCT) as recommended by[47] using ASTM E399-09 testing standard along with a data reduction technique based on FEA.

3. Materials and Method

3.1. Materials

3.1.1. Fibers

In this experimental investigation chopped acacia tortilis fiber and plain-woven glass fiber were used as reinforcement as shown in Figures 12 and Figure 13. Plain-woven glass fiber was purchased from World Fiber Glass and Waterproofing Engineering, Addis Ababa, Ethiopia. Acacia tortilis fiber was collected from different live trees in Shewarobit, the fiber was first extracted from the bark of branches of the acacia tortilis tree. It was chopped with the help of scissors.

Due to its good balance between cost and performance, high strength, stiffness, good insulation properties as well as an excellent resistance to chemicals, moisture, and heat, E-glass fiber is mostly used as a reinforcement fiber[65].

Acacia tortilis is one source of natural fiber-reinforced composite and is suitable for use as a reinforcement in thermoset polymers[20]. due to its abundance, cheapness, low density, and good competitive strength with other natural fibers[6].

Table 2 Properties of Acacia Tortilis Fiber *[32]*

material	density	Tensile strength MPa	Tensile modulus MPa	Elongation, %
Acacia Tortilis Fiber (AT)	0.906	71.63	4.209	1.33

Figure 12 woven glass fiber

(a) *(b)*

(c)

Figure 13 (a) layer by layer separated Acacia Tortilis fiber (b) unseparated Acacia Tortilis fiber (c) chopped AT fiber

3.1.2. Matrix

For this experimental investigation, unsaturated polyester resin is used as a matrix material and the catalyst for curing the resin was purchased from World Fiber Glass and Waterproofing Engineering in Addis Ababa, Ethiopia.

Polyester resin has wide applications in diverse structural and non-structural application sectors such as construction, aircraft manufacturing, automotive, marine, packaging, furnishings, and textiles. They have the capability to take on the desired shape, whether applied wet or dry, and they exhibit rapid drying. Additionally, polyester resins resist stretching and wrinkling/folding, and they offer durability against shrinking, and abrasion, while maintaining a colorless and transparent quality[18]. for these benefits of the polyester resin and its compatibility with acacia tortilis fiber [32] and with glass fiber[41], I used it as a matrix material for this experimental investigation. Typical properties of unsaturated polyester are presented in below Table 3.

Table 3 properties of unsaturated polyester [6], [66]

Properties	**Values**
Density (g/cm^3)	1.2 g/cm^3
Tensile strength (MPa)	50 MPa
Tensile modulus	3000 MPa
Elongation (%)	2.5
Poisson's ratio	0.38
Shear modulus	2460 MPa

3.1.3. Utility materials

For this experimental investigation Pellet sodium hydroxide (NaOH) (figure 14 a) and distilled water (figure 14 b) were used for the treatment of AT fiber. For easy depart of the prepared composite material from the mold surface Wax (figure 14 c) were used as a mold release agent and all these materials were purchased from local markets in Addis Ababa, Ethiopia.

(a) (b) (c)

Figure 14 (a) Sodium Hydroxide (NaOH) pellet (b) distilled water (c) Wax-mold release agent

3.2. Experimental Methods

3.2.1. Fiber Processing

3.2.1.1. Fiber extraction process

After the Acacia tortilis fiber was collected, the soft inner part of acacia tortilis bark that is the fiber by itself was separated from the hardcover, then the fiber was retted/soaked in water for 24 days as suggested by a previous study [67] for easy separation of the layers of the fiber as shown in figure 16 (a). During the water retting process, the water was changed every 5 days. Then the soaked fiber was washed so many times with fresh water and separated the layers of the fiber before being allowed to dry in open air for 1 week. Then the dried fiber was treated with alkaline treatment and further extraction processes were done.

(a)

(b)

(c)

Figure 15 (a) fiber soaking with water (b) fiber after water retting (c) fiber under drying in open air

3.2.1.2.Chemical Treatment of Fiber

The chemical treatment of the fiber was done using 10% NaOH solution. The steps followed during the alkaline treatment of fiber are:

a) Prepare the final extracted and dried acacia tortilis (AT) fiber for the treatment.
b) Determine the required amount of sodium hydroxide (NaOH) pellet and distilled water according to rule of mixture for 10% NaOH concentration.
c) Measuring the amount of NaOH and mix with distilled water and stir.

d) Soak the fiber at room temperature in a bucket and cover it with a plastic sheet to create a vacuum inside the bucket (figure 16 (a)). and leave it in the solution for 4 hours as suggested in the previous study [68].
e) Wash the soaked fiber several times with distilled water and then with fresh water to neutralize the alkaline solution.
f) Then dry the treated fiber for five days [32].

(a) (b)

Figure 16 (a) AT fiber under NaOH solution treatment (b) AT fiber after treatment and dried

3.2.2. Specimen Preparation steps

3.2.2.1.Fabrication of laminate composite panels

The hand lay-up method followed by the compression molding technique is used in this composite panel's fabrication. There are four different composite panels are fabricated these are 1 pure glass fiber (G-G-G-G-G-G-G) composite panel, 2 hybrids (G-AT-G-AT-G-AT-G, G-G-AT-AT-AT-G-G) composite panels, and 1 pure acacia tortilis fiber (AT-AT-AT-AT-AT-AT-AT) composite panel. The dimension of fabricated composite panels is$250mm * 200mm * 5.6mm$. the total volume fraction of the fiber used in this composite fabrication is 0.3 as suggested by [58] the total number of layers in all fabricated composite panels is kept as 7. In the two-hybrid composite panels, the outer layers are glass fiber to improve the moisture absorption resistance property of the composite since glass fiber has better moisture absorption resistance properties.

3.2.2.2. Mass-Volume Content of Fiber and Matrix of the Composite

In the hybrid composite laminate fabrication process the first step and task to be done is determining the mass and volume percentage/content/ of the constitutes (fibers & matrix). The properties of hybrid composite laminate elements are determined and relied on the values of fibers and matrix fraction presence [69]. The results of calculated parameters using the below equations are used in the composite laminate preparation.

$$Density\ of\ composite, \rho(g/cm\text{^}3) = \rho_f v_f + \rho_m v_m \ldots\ldots\ldots\ldots\ldots\ldots\ldots \textit{equation 3.1}$$

$$Mass\ of\ composite, m(g), m = \ \rho_c * V_c \ldots\ldots\ldots\ldots\ldots\ldots\ldots\ldots\ldots \textit{equation 3.2}$$

$$Volume\ of\ glass\ fiber\ (cm^3) = v_g * V_c \ldots\ldots\ldots\ldots\ldots\ldots\ldots\ldots\ldots\ldots \textit{equation 3.3}$$

$$mass\ of\ glass\ fiber(g) = \rho_g * V_g \ldots\ldots\ldots\ldots\ldots\ldots\ldots \textit{equation 3.4}$$

$$volume\ of\ acacia\ tortilis\ fiber(cm^3) = V_f * V_c \ldots\ldots\ldots\ldots\ldots \textit{equation 3.5}$$

$$Mass\ of\ AT\ fiber(g) = \rho_{AT} * V_{AT} \ldots\ldots\ldots\ldots\ldots\ldots\ldots\ldots\ldots \textit{equation 3.6}$$

$$Volume\ of\ polyester(cm^3) = v_m * V_c \ldots\ldots\ldots\ldots\ldots\ldots\ldots\ldots \textit{equation 3.7}$$

$$Glass\ fiber\ wt\% = \frac{m_g}{m_c} \ldots\ldots\ldots\ldots\ldots\ldots\ldots\ldots \textit{equation 3.8}$$

$$total\ mass\ of\ the\ composite(g) = m_{AT} + m_g \ldots\ldots\ldots\ldots\ldots\ldots\ldots\ldots \textit{equation 3.9}$$

Where:

ρ_f-density of fiber

v_f- Volume fraction of fiber

V_f-volume of fiber

V_{AT}-volume of acacia tortilis fiber

ρ_m-density of matrix

v_m-volume fraction of matrix

ρ_c-density of composite

V_c-volume of composite

m_g-mass of glass fiber

m_{AT}-mass of acacia tortilis fiber

ρ_{AT}-density of acacia tortilis fiber

V_{AT}-volume of acacia tortilis fiber

m_c-mass of composite

Table 4 constant and calculated parameters value

Constant parameter		Calculated parameters	
Parameters	value	Parameters	value
$Total\ volume\ fraction\ v_f$	$\mathbf{0.3}$	$Density\ of\ composite, \rho(g/cm\text{^}3)$	$\mathbf{1.602 g/cm^3}$
$Density\ of\ AT\ fiber$	$\mathbf{0.906\ g/cm^3}$	$Mass\ of\ composite, m($	$\mathbf{448.56 g}$
$Density\ of\ glass\ fiber$	$\mathbf{2.54\ g/cm^3}$	$Volume\ of\ polyester, V_{poly}$	$\mathbf{196 cm^3}$
$Density\ of\ polyester\ resi$	$\mathbf{1.2 g/cm^3}$	$Mass\ of\ polyester, m_{poly}$	$\mathbf{235.2 g}$
$Volume\ of\ composite$	$\mathbf{280 cm^3}$	The volume and mass calculations of fibers for each type of laminate are annexed in the appendix.	

The relative percentage of the constituents used in this composite fabrication is summarized in the table below (Table 5) the details of the calculation of these constituents are annexed in appendix A. The four composite laminate plies configurations were presented in Figure 17 (a)-(d).

AT
AT
AT
AT
AT
AT
AT

(a) Pure AT laminate

G
AT
G
AT
G
AT
G

(b) Hybrid (H1) laminate

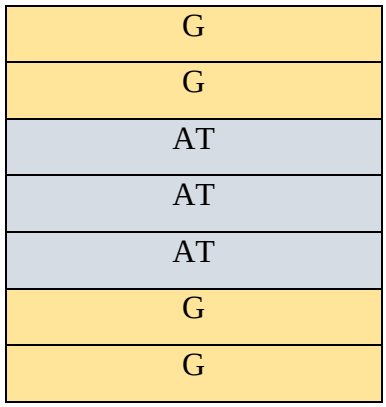

(c) Hybrid (H2) laminate

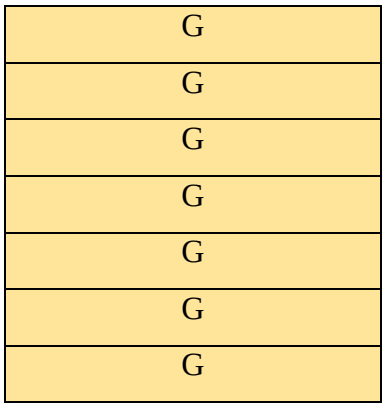

(d) Pure Glass laminate

Figure 17 composite plies configuration for all four composite laminates

Table 5 summarized relative percentage of constituents of the composite panels

Laminates	Layers sequence	Fiber volume fraction (V_f)		Calculated fiber mass fraction (wt%)		Volume fraction of unsaturated polyester resin
		AT	G	AT	G	
Pure G	G/G/G/G/G/G/G	0	30	0	47.57	70
Hybrid (H1)	G/AT/G/AT/G/AT/G	13	17	12.91	29.57	70
Hybrid (H2)	G/G/AT/AT/AT/G/G	13	17	12.91	29.57	70
Pure AT	AT/AT/AT/AT/AT/AT/AT	30	0	34.12	0	70

The steps followed during the composite panel's fabrication are:

i. Measuring the required amount of final prepared AT fiber and unsaturated polyester resin using digital balance (shown in figure 18 a) also in parallel make ready the final prepared glass fiber.

ii. Clean and varnish all sides of the 250mm*250mm rectangular metal mold (figure 18 b) using Honey Wax 250 wax mold release agent.

iii. Use 5.6mm (in depth) rectangular steel rods from the sides of the mold that are used for limiting the thickness of the composite panels under pressing.

iv. Mix the resin with its hardener with the mixture ratio of 10:1 as per suggestion of the manufacturer and stir it continuously until we get complete mixture.

v. Wetting the bottom surface of the mold with adequate amount of resin. Then place the reinforcing fibers successively along with applying the required amount of resin uniformly using brush for the respected composite panel until all the 7 layers are done. A spike roller was used to uniformly distribute the resin as well as remove trapped air.

vi. After successfully placed all the layers, close the mold with its female upper cover and solidify the prepared composite by pressing the mold using a hydraulic press machine (figure 20).

(a) (b)

Figure 18 (a) digital balance used for measuring the fiber mass, (b) rectangular steel mold with its female upper cover

Figure 19 setup and hand lay-up fabrication of composite laminates

Figure 20 solidification processes using a hydraulic press machine

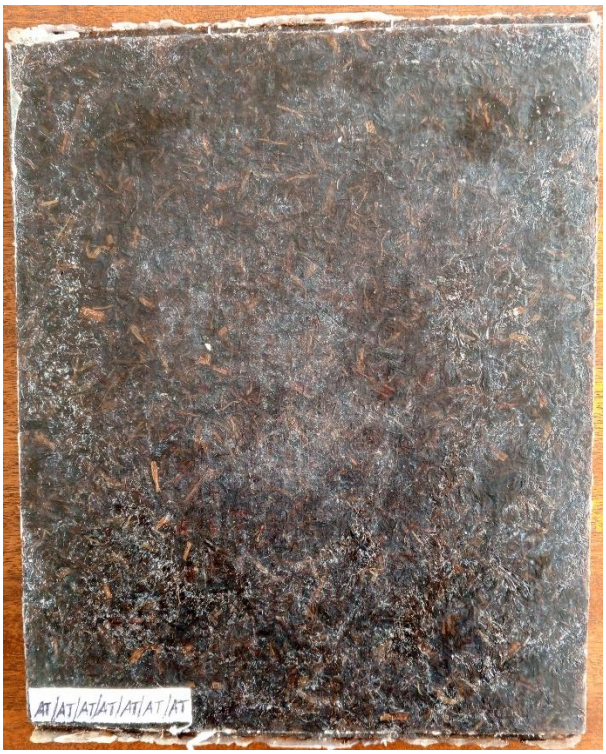

Figure 21 all fabricated composite panels

3.2.2.3.Specimen cutting processes

From the fabricated composite laminate panels specimens were prepared by cutting using hack saw and also a sharp knife for surface finishing in order to evaluating the intralaminar fracture toughness parameters & critical energy release rate. The selected compact tension (CT) specimen geometry was a doubly tapered compact tension specimen (2TCT). Since it showed minimum values for failure indices [55].

A total of 6 doubly tapered compact tension (2TCT) specimens were prepared from each fabricated composite laminate panel, 5 of them were used for testing. The configuration and dimensions of the specimen are shown in the below schematic diagram (Figure 22).

The prepared composite laminate panels are first marked with the 2TCT (doubly tapered compact tension) specimen geometry and dimension as shown in Figure 24. Then drilling operations were performed.

After cutting the chamfers, the initial opening (v-shaped with a 4mm at its mouth and ends for a length of 33mm) was performed successively. An additional 1mm in crack length was made using a blade. The scale was drawn on all specimens of the four composite panels which are ready to conduct an intralaminar fracture toughness test as shown in Figure 24.

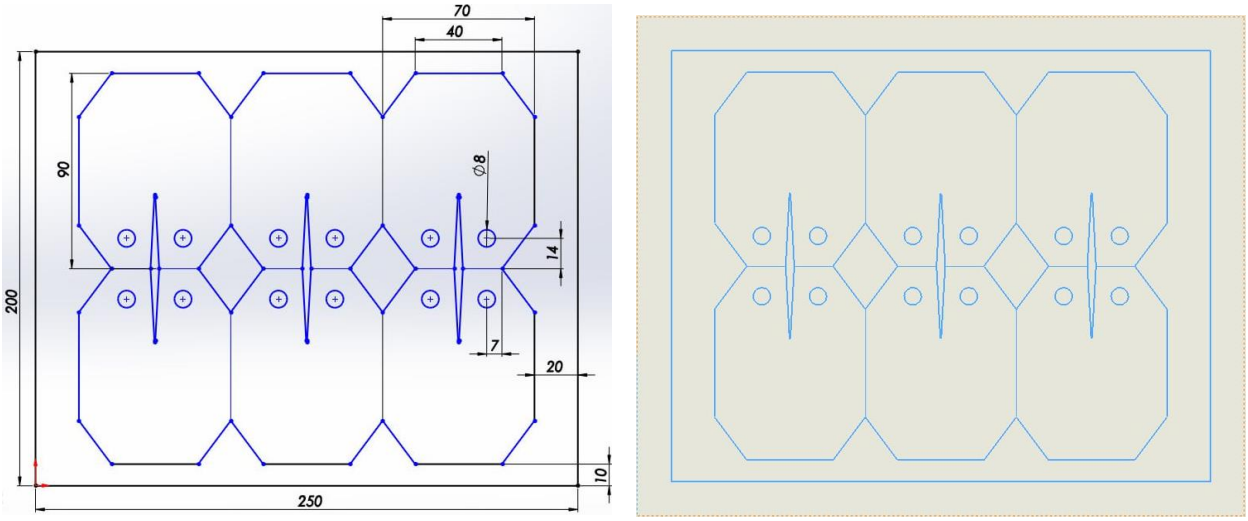

All dimensions are in mm.

Figure 22 schematic diagram showing configuration & dimensions of the 2TCT specimens

(a)

(b)

Figure 23 (a) specimens cutting using hack saw (b) drilling composite laminates

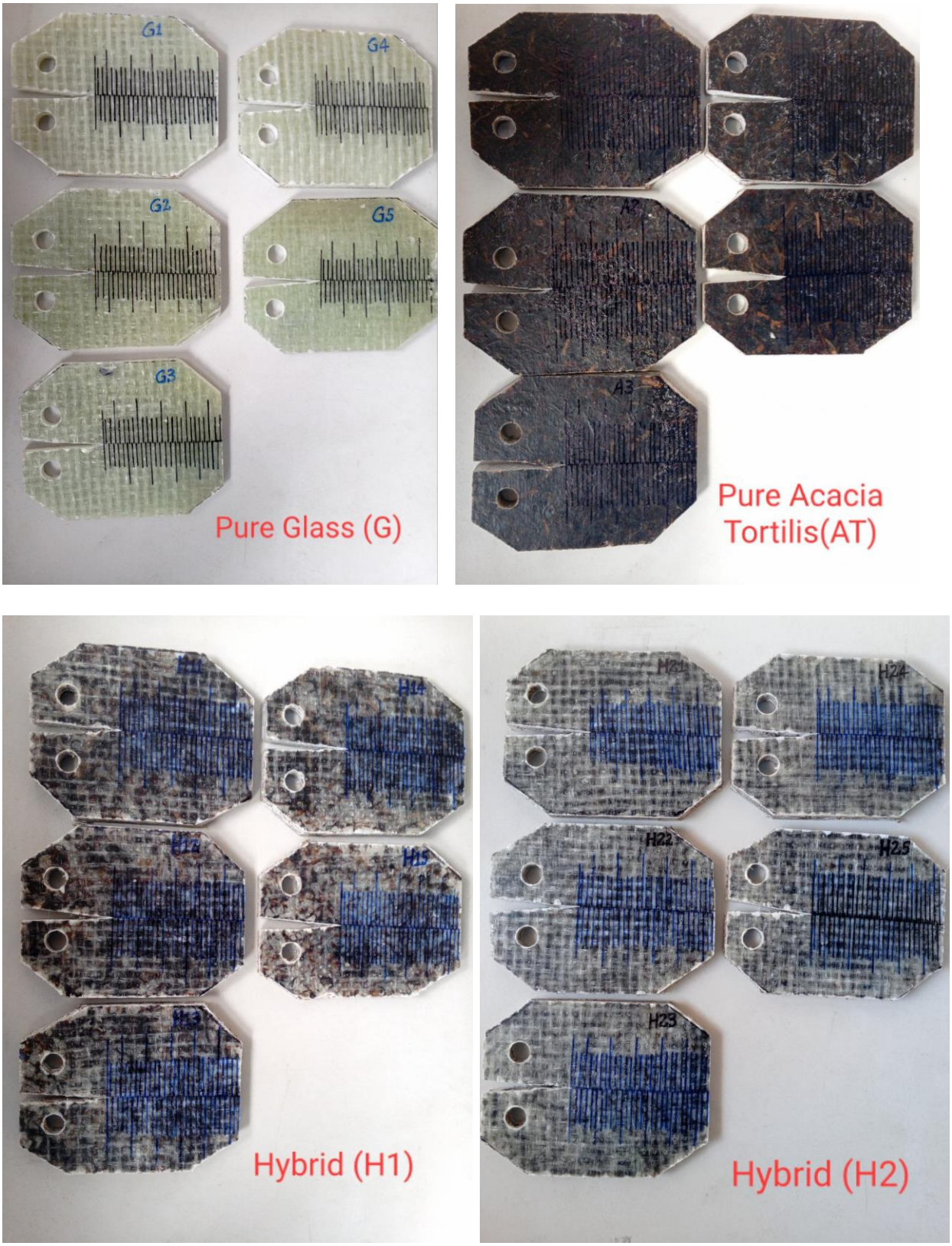

Figure 24 prepared specimens ready for conduct a test

3.2.3. Test procedure and setups

The Mode-I tensile test was performed on the prepared 2TCT (doubly tapered compact tension) specimens of all composite laminates at Addis Ababa Science and Technology University using Universal Testing Machine (UTM) of model WDW-100S and serial number Q21101. The UTM has a test load capacity of up to 100 KN and a crosshead speed of 0.5 mm/sec.

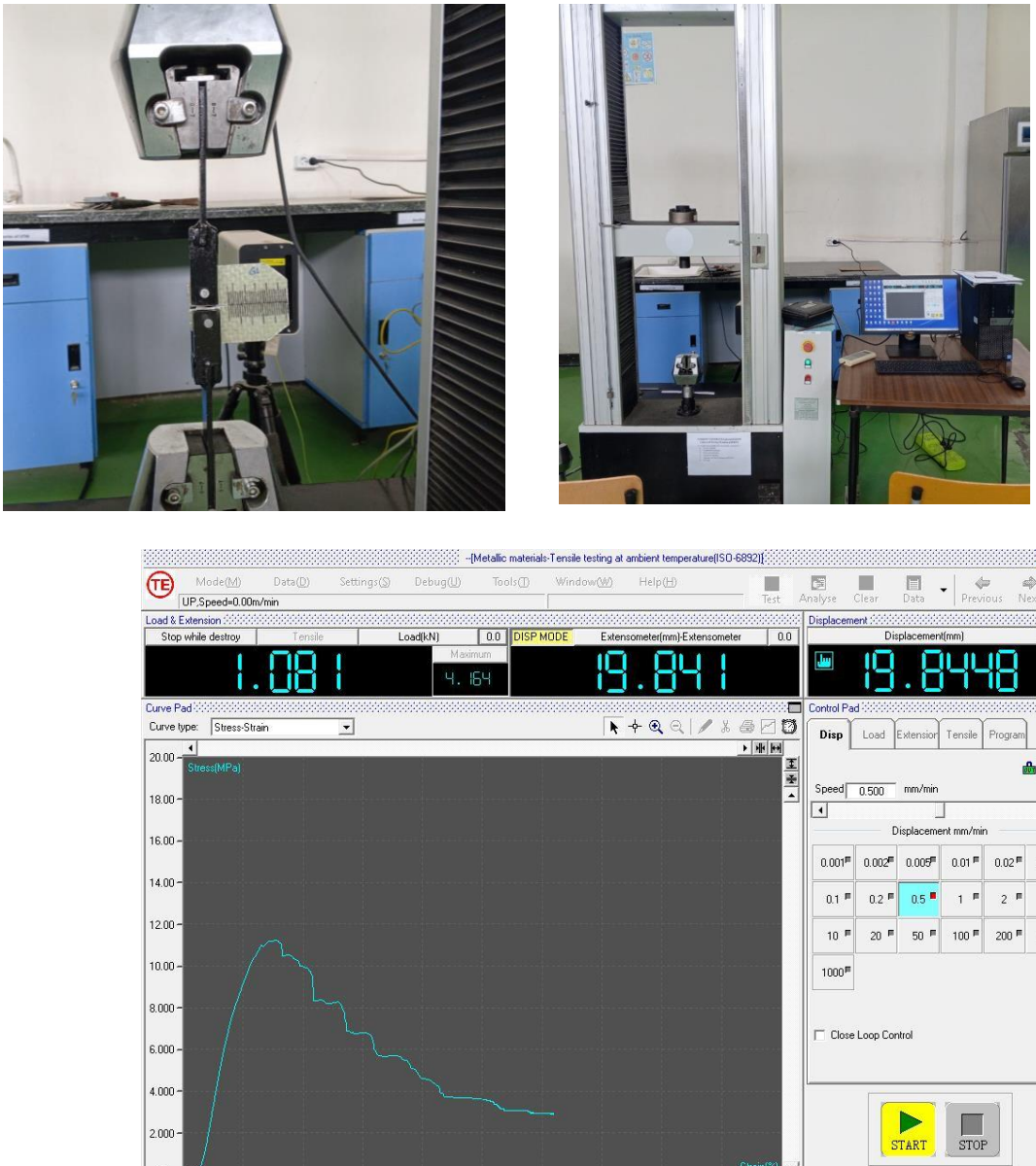

Figure 25 Universal Testing Machine (UTM) with loading setup and image of data recording computer window for trial.

The test procedure and steps were performed as per the standard of ASTM E399. In order to acquire data from the machine during testing, data acquisition software was used and a specimen fixture shown in figure below (figure 26) to load and setup the specimens in to the machine is used. During the testing the load was continuously applied from the dynamometer load cell until the specimen fails.

Figure 26 specimen's fixture with pins

3.3. FE Computation

3.3.1. Data reduction

To determine the fracture toughness of orthotropic materials, many literatures and researchers have used ASTM D5045 [54], which is for plastic materials, and some others have used ASTM E399 [53], which is even valid for metallic materials. Although determining the fracture toughness of a material requires attention.

Both considerations assume that the material is isotropic. Due to this assumption, a difference was observed in the fracture toughness result using FEA and using the stress intensity factor equation. To resolve this difference, Pinho et al. developed a more accurate data reduction method for determining the fracture toughness of a composite material [48]. Using this developed data reduction formula (equation 3.10) and the ASTM E399-09 standard, the mode I critical energy release rate can be evaluated for the prepared 2TCT samples.

$$G_{IC} = \left(\frac{P_c}{t}\right)^2 (C_3 a^3 + C_2 a^2 + C_1 a + C_0) \ldots\ldots\ldots\ldots equation\ 3.10$$

$$Where, \quad Pc - experimental\ load\ at\ specific\ propagated\ crack\ length\ a$$

$$t - thickness\ of\ the\ specimens$$

$$C_i - polynomial\ coefficients\ can\ be\ determined\ from\ FEA$$

The normalized energy release rate f (a), obtained from the J-integral near the crack tip of composite specimens of unit thickness under unit load, is expressed using a polynomial expression in the above equation. The normalized energy release rate values at each crack length (as shown in Appendix B) were computed using Abaqus/CAE 2017. After having the f (a) at each crack length the polynomial coefficients Ci's were determined using MATLAB 2024b in a range of crack length a.

3.3.2. Experimental load Determination

To calculate the G_{IC} value of composite laminates, it is first necessary to obtain the maximum/maximum load from the load-displacement curve from the experimental data. As suggested in ASTM Standard Test Method E-399-09 [52] the maximum/peak/ can be determined by plotting the secant OP_5 (to determine the conditional value of P_Q) through the origin O with a slope of $(P/V)_5$ equal to 0.95(P/V)o, where (P/V)o is the slope of the tangent OA to the initial part of the graph as shown in Figure 27. Then the load P_Q is determined as; Type I (if the load at every point of the record that precedes P_5 is less than P_5, then P_5 is P_Q), Type II, and Type III (if there is a maximum force before P_5 that exceeds it, then this maximum force is P_Q).

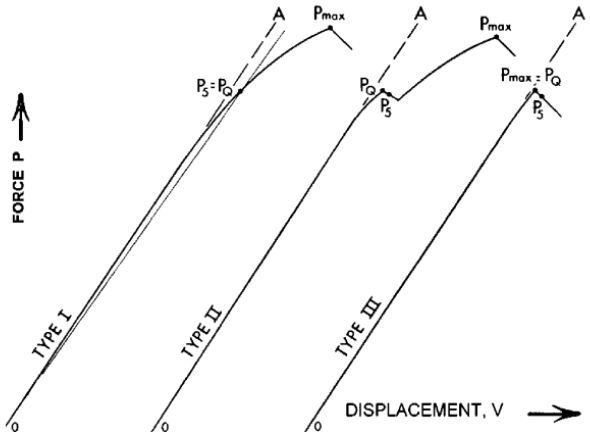

Figure 27 principal types of force-displacement curves [52]

3.3.3. FEA for Polynomial Coefficients Determination

The finite element analysis was performed by modeling a half-crack 3D deformable shell planar model using Abaqus (CAE 2016, V 6.14-5) since the 2TCT specimen is symmetrical in geometry. the geometry was modeled as per the recommendation by [47]. The model has meshed using uniform square 8-node (S8R5) elements with a finer mesh applied at the load application points and crack tip.

The displacement of the lower right node was constrained in the x direction and a symmetry boundary condition was applied in the plane of symmetry as shown in Figure 28. A 2TCT specimen model was developed using unit thickness and a tensile unit load was applied at the top of the pinhole to attempt to open the initial crack. FEA was performed to evaluate the J-integrals of five contours around the crack tip by defining the location of the crack point at its tip and determining the direction of the crack's propagation along the anticipated crack plane.

For this setup, the FEA can be repeated to determine the normalized energy release rate (J-integral) values for each sample of composite laminates for a crack length of 20mm to 64mm with a step of 1mm. To do this repeated FE analysis, a Python code was used. By changing the values of crack length (a), elastic material properties of a composite laminate, and with a selected maximum and minimum mesh size factors in the Python code and running it in the Abaqus to obtain the J-integral values of a specific composite laminate.

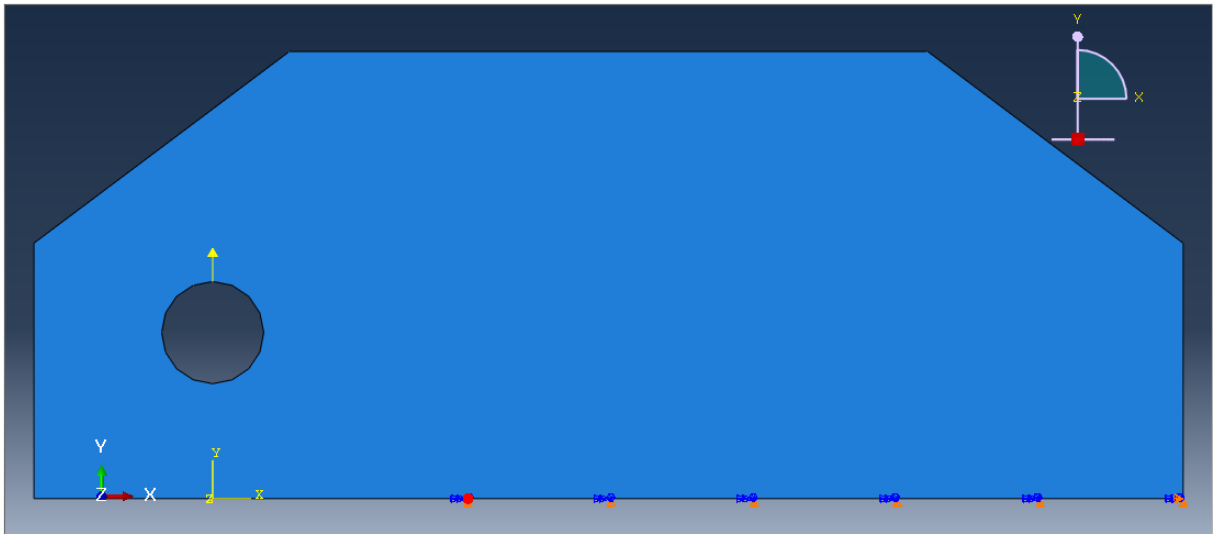

Figure 28 Abaqus FE symmetric model of 2TCT specimen with a crack

As presented in table 6 below, the elastic properties of the Acacia Tortilis/ Polyester were taken from [20], and the in-plane shear modulus and major poison's ratio were taken from [70]. The elastic properties , in-plane shear modulus and major poison's ration values of Glass/Polyester lamina were taken from [71], [72]

Table 6 elastic properties of AT/Polyester and Glass/Polyester Lamina[70] [20],[71],[72]

Lamina	Elastic Modulus (GPa)			**Major Poisson's ratio**
	E1	E2	G12	(v_{12})
AT/Polyester	3.80	3.80	2.46	0.38
Glass/Polyester	11.3	11.3	4.2	0.27

By having the elastic properties of the laminas, the elastic properties of composite laminates were evaluated using the composite lamination theory as shown in Table 7.

Table 7 Elastic properties of the composite laminates (using lamination theory mentioned in [73])

Laminates	Elastic Modulus (GPa)			**Major Poisson's ratio**
	E1	E2	G12	(v_{12})
Pure AT	3.80	3.80	2.46	0.38
Hybrid (H1)	8.104	8.104	3.454	0.2936
Hybrid (H2)	8.104	8.104	3.454	0.2936
Pure Glass	11.3	11.3	4.2	0.27

3.3.4. Mesh Convergence Test

By considering different mesh size factors and level of refinement the mesh convergence test was done for this FEA approach of the study. In order to control the level of mesh refinement two mesh size factors, minimum size factor and maximum size factor were set. For better accuracy of a result, the minimum size factor enables to manage the mesh refinement around crack point and load application point where as the maximum size factor used to manage the mesh refinement of the geometry/model away from the two points.

The symmetry meshed geometry of 2TCT finite element model with different mesh type (coarse mesh, intermediate mesh, and Fine mesh) is shown in figure 31.

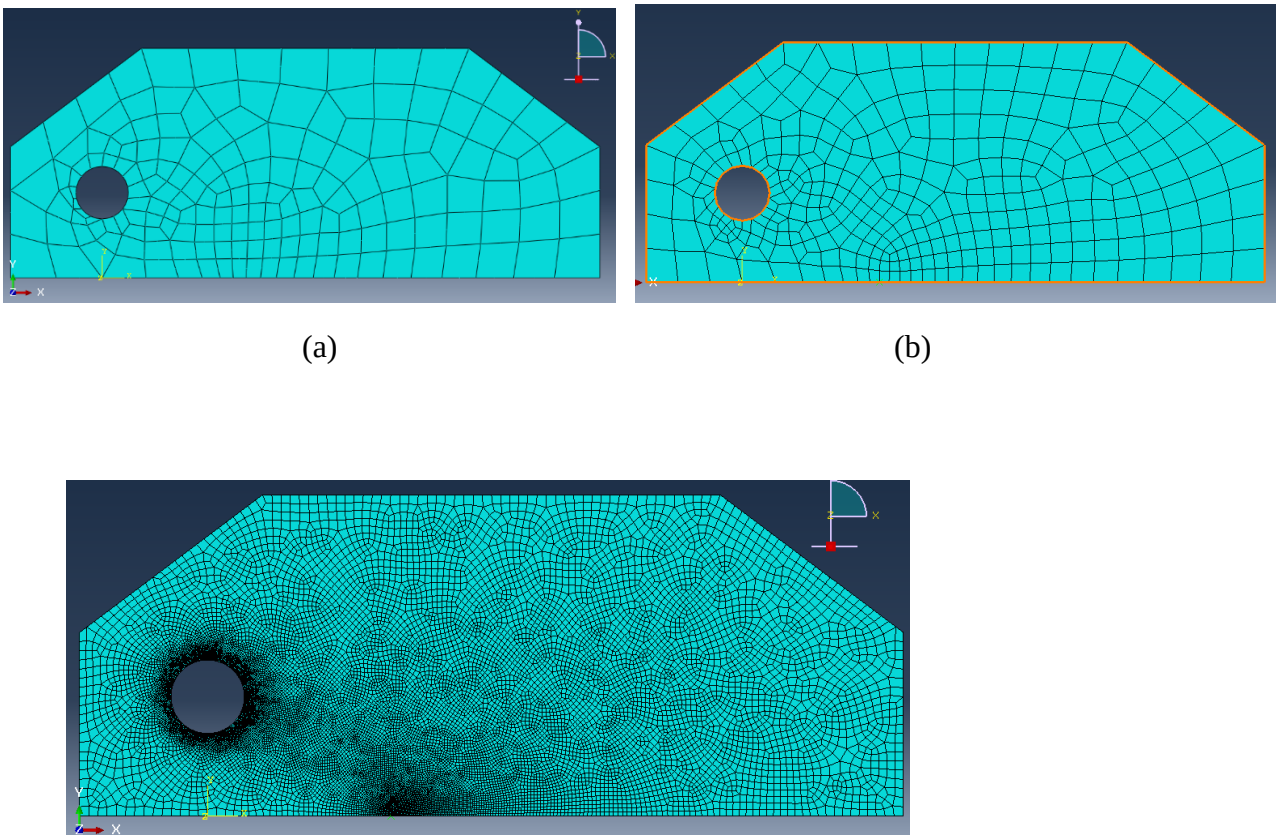

(a) (b)

(c)

Figure 29 Mesh refinement levels of a symmetry 2TCT FE model (a) coarse mesh, (b) intermediate mesh, and (c) fine mesh

The minimum and maximum mesh size factors for the above three mesh refinements (coarse mesh, intermediate mesh, fine mesh) are presented in Table 8.

Table 8 coarse, intermediate, and fine mesh refinements with their max. And min. size factors

Level mesh refinement	Number of elements	Max. size factor (mm)	Min. size factor (mm)
Coarse mesh, figure 31(a)	173	7	2
Intermediate mesh, figure 31 (b)	546	4	1.1
Fine mesh, figure 31 (c)	17564	1	0.1

The mesh convergence test was done by changing the value of maximum and minimum mesh size factor values in the python code for different level of mesh refinement and then by run it in abaqus the J-integral (normalized energy release rate), number of element, and total CPU time taken were obtained. By evaluating the percentage error for these level of refinements level 7 (figure 30), with maximum mesh size factor of 1mm and minimum mesh size factor of 0.2mm, and with percentage error of 0.0041 was selected for the analysis. By having the mesh convergence data's (Table 9) at different level of refinement the mesh convergence plotted as presented in Figure 33.

Table 9 levels of mesh refinement data's for mesh convergence test

Level of mesh refinement	Max. size factor (mm)	Min. size factor (mm)	No. of elements	Total CPU time (Sec)	Normalized energy release rate (m^2/kJ)	Percentage error (%)
1	7	2	173	0.2	7.1706E-05	0.1045
2	6	1.7	226	0.3	7.1727E-05	0.0753
3	5	1.4	334	0.4	7.1732E-05	0.0683
4	4	1.1	546	0.5	7.1747E-05	0.0474
5	3	0.8	954	0.7	7.1757E-05	0.0334
6	2	0.5	2190	1.7	7.1769E-05	0.0167
7	1	0.2	10235	7.9	7.1778E-05	0.0041 (***Selected)***
8	1	0.1	17564	14.1	7.1781E-05	Ref.

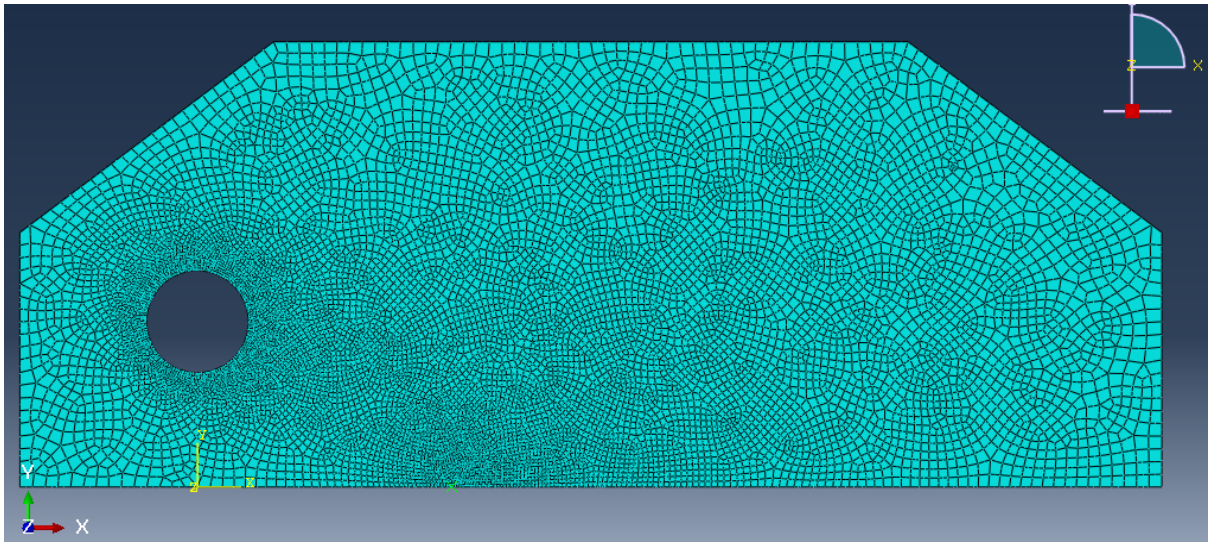

Figure 30 selected level of mesh refinement-level 7

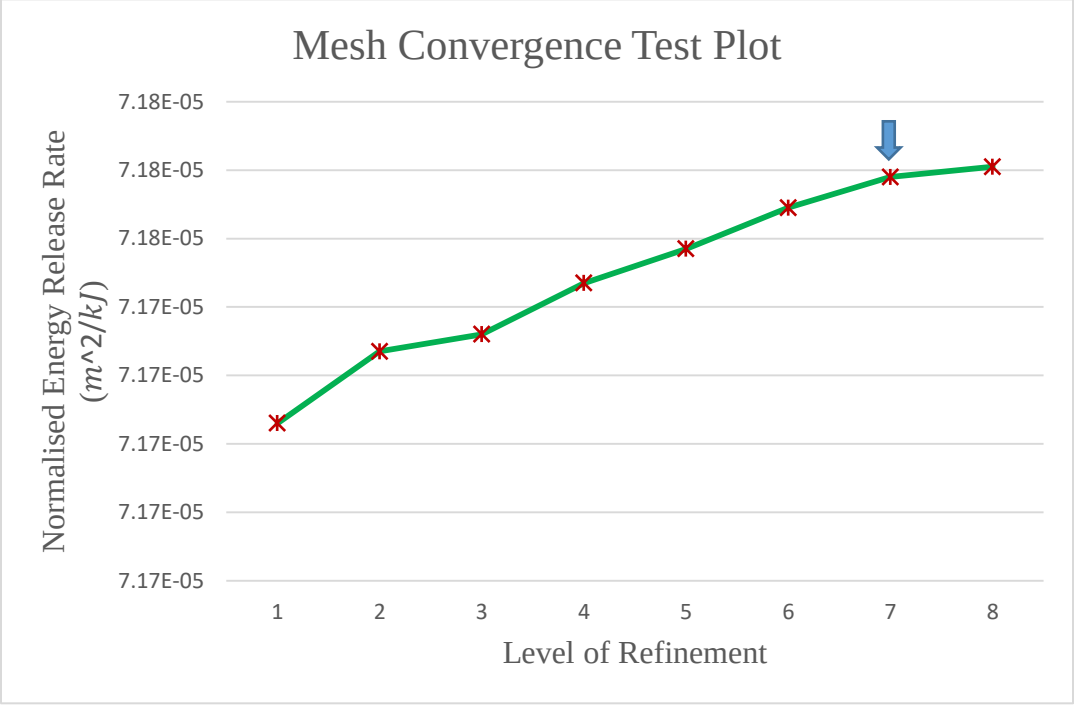

Figure 31 Mesh convergence test plot (arrow locates the convergence point)

4. Results and Discussion

4.1. Experimental Results

4.1.1. Load vs. Displacement Graph

As discussed and explained earlier in the test setup and procedure section, the intralaminar fracture toughness test under Mode-I was performed using UTM. From the result, the load vs. displacement graph for each composite laminate (each having 5 specimens) is presented in Figure 32 (a)-(d) below.

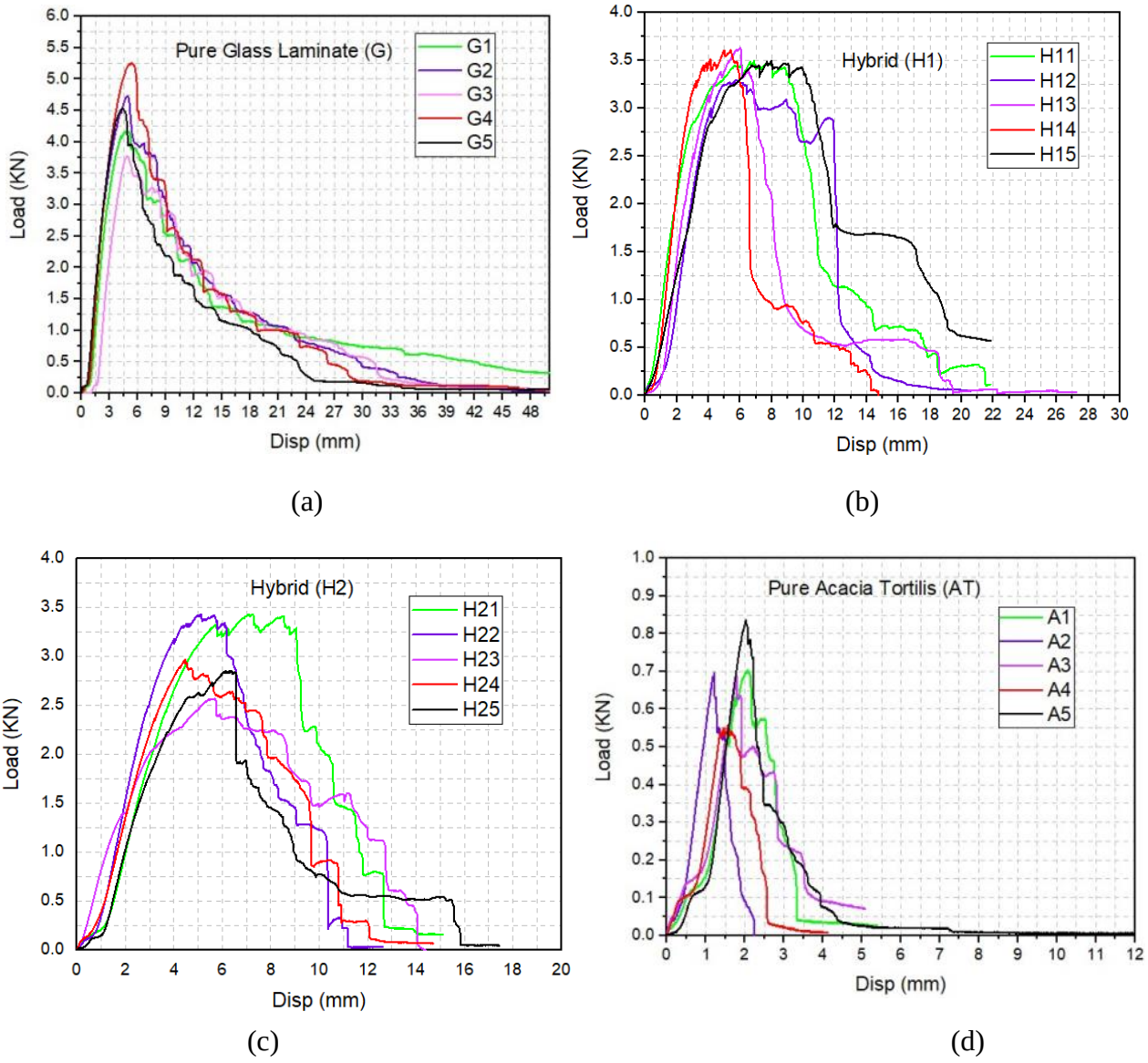

Figure 32 load vs. displacement curves (a) for pure glass laminate (G), (b) for Hybrid (H1), (c) for Hybrid (H2), (d) for pure acacia tortilis (AT) laminate

The load-displacement curves for pure glass fiber laminate (figure 32a), Hybrid H1 (figure 32 b), Hybrid H2 (figure 32c), and pure acacia tortilis (Figure 32d) can be discussed in five phases.

At phase I (pre-loading) - The upper and lower loading pins compress and create micro penetrations in the specimen holes to bring system compliance.

At phase II (Elastic phase) - The load is nearly proportional to the displacement, during this phase, deformations are almost reversible. In essence, the system behaves elastically under these conditions. The average peak load of pure AT, hybrid (H1), hybrid (H2), and pure glass was 0.696 kN. 3.28 kN, 3.05 kN, and 4.49 kN respectively. The average stiffness of pure AT, hybrid (H1), hybrid (H2), and pure glass was 0.32 kN/mm, 0.75 kN/mm, 0.62 kN/mm, and 0.92 kN/mm respectively.

At phase III (damage initiation phase or transition phase) - The curves begin to deviate slightly from linearity and show sudden changes near the maximum load. During this stage, some fibers near the crack tip begin to break and separate from the matrix, accompanied by audible clicking sounds. However, no visible crack growth was detected during this phase.

At phase IV (damage propagation phase) - a continuous sudden drop and stabilization of the load was observed, with the load curve resembling a series of steps. The sudden drop in load results from unstable crack propagation through matrix-rich regions, while stabilization occurs when the crack propagates steadily through fiber-rich regions. Crack growth slows when the crack tip encounters fibers or fiber bundles, but once these fibers are broken and the crack reaches matrix-rich regions, it propagates rapidly. The gradual nature of damage propagation, rather than catastrophic failure, is one of the key advantages of these natural fiber composite materials.

At phase V (final failure phase)- Along with tensile failure near the crack tip, vertical compressive failure modes were also observed in the compressive failure zone as shown in figure 38(a), including fiber knotting, matrix crushing, and delamination. The load-displacement curves of these composites exhibit a pattern like the curve mentioned in [74].

4.2. FE Computational result

4.2.1. Determination of Polynomial coefficients

As explained in the FEA section of methodology, the FE analysis was computed using Abaqus (CAE 2016, V 6.14-5). The model was developed with a half-symmetrical geometry of thickness 1mm and the analysis was calculated by applying a unit load of 1KN. By computing the polynomial coefficients at a unit load from the FEA, the critical energy release rate value was evaluated using equation 3.10 and as mentioned in [47] at the experimental load at a specific crack length.

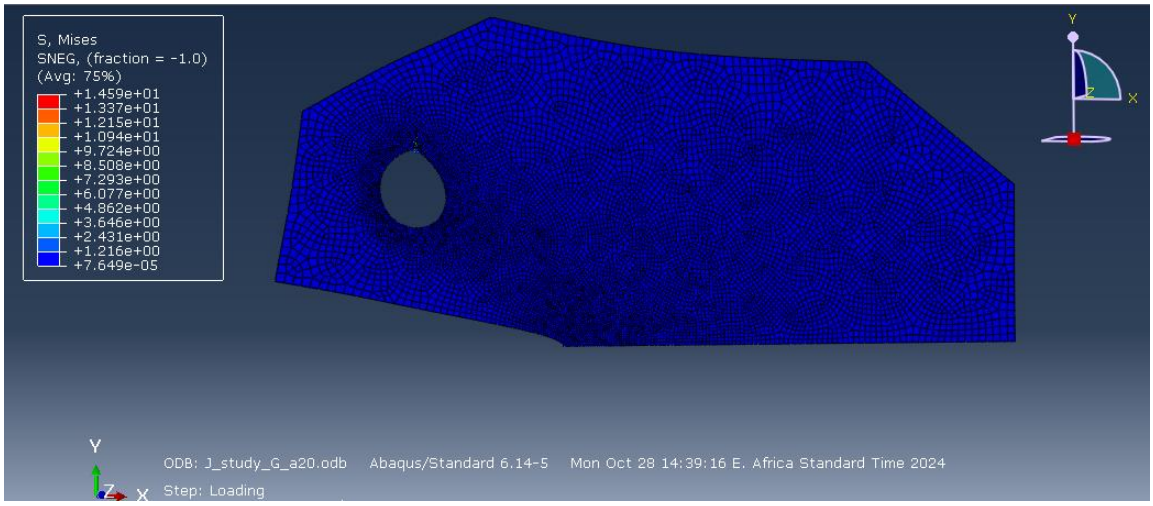

(a)

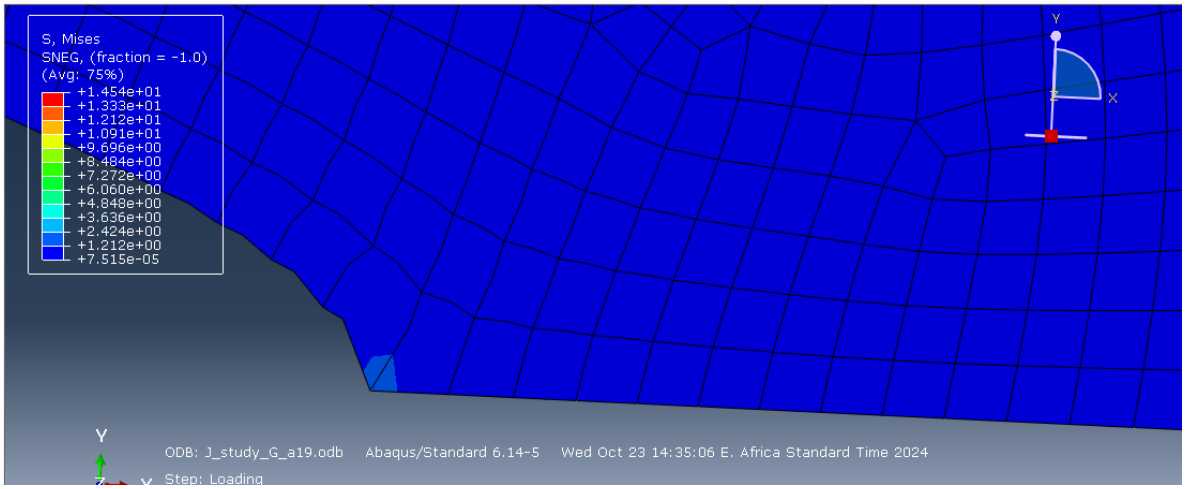

(b)

Figure 33 (a), Von-misses stress distribution of 2TCT specimen (b), magnified view for crack tip

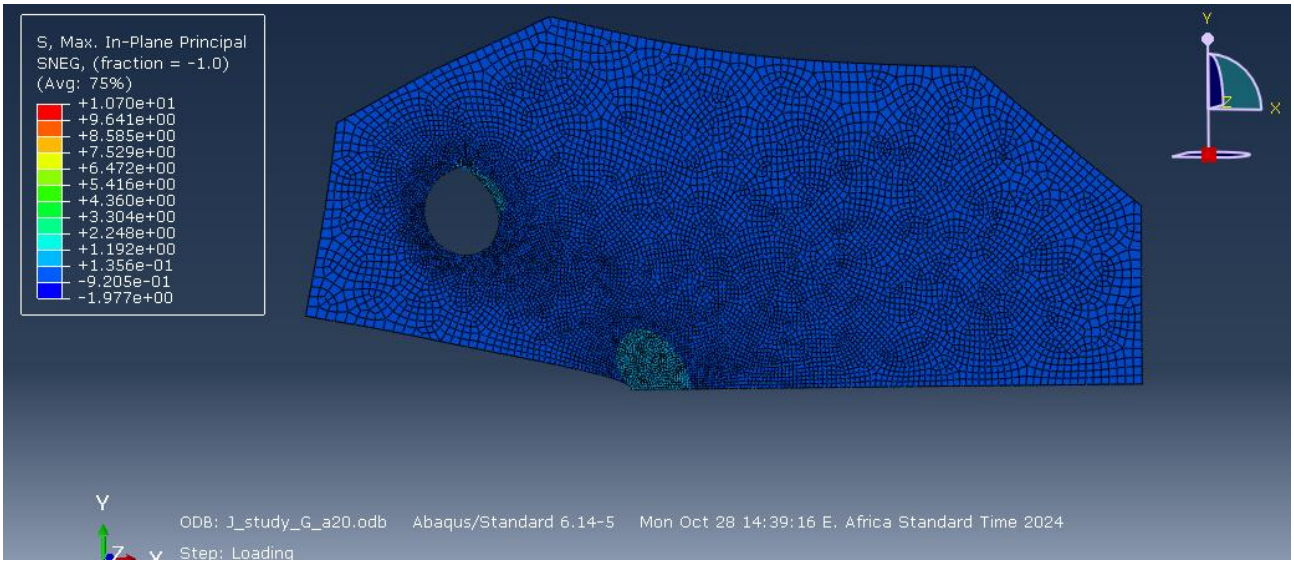

(a)

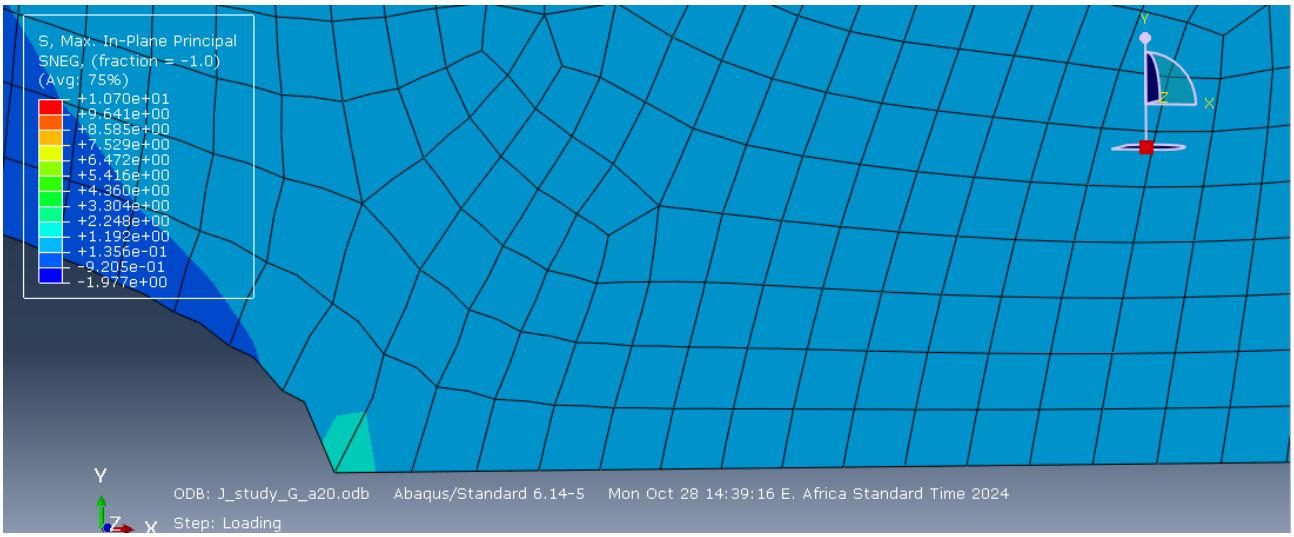

(b)

Figure 34 (a), in-plane principal stress distribution of 2TCT specimen (b), and magnified view for crack tip

As shown in figure 33 and figure 34, the von-misses and in-plane principal stress distribution concentrates around the crack tip of the 2TCT specimen. It is a desirable condition to promote the crack propagation along the anticipated crack plane.

Using the python code and editing the elastic properties of laminates as well as the crack length a from 19mm-64mm under selected maximum and minimum mesh size factor values 1mm and

0.2mm respectively, the normalized energy release rate/J-integral value/ were computed for each crack length as shown in (Appendix B).

After having the normalized energy release rate f(a) values at each crack length for each composite laminates, the polynomial coefficients were computed by interpolating in MATLAB R2024a (curve fitting APP) for a range of crack lengths as mentioned Blanco et al. [47] As shown in Table 10 below.

Table 10 interpolated polynomial coefficients for all composite laminate

Crack length ranges	C_3	C_2	C_1	C_0	**Interpolation Error(in %)**
For Pure AT Laminate					
$19 \leq a \leq 30$	9.84E-09	-5.12E-07	1.60E-05	-7.35E-05	<0.02
$30 \leq a \leq 40$	3.79E-08	-3.13E-06	9.80E-05	-9.31E-04	<0.03
$40 \leq a \leq 50$	2.19E-07	-2.57E-05	1.038E-03	-1.40E-02	<0.04
$50 \leq a \leq 60$	2.64E-06	-4.04E-04	2.08E-02	-3.56E-01	<0.42
$60 \leq a \leq 65$	2.75E-05	-4.88E-03	2.89E-01	-5.75	<0.023
For Pure Glass Laminate					
$19 \leq a \leq 30$	3.76E-09	-1.89E-07	5.81E-06	-2.12E-05	<0.015
$30 \leq a \leq 40$	1.52E-08	-1.25E-06	3.91E-05	-3.69E-04	<0.03
$40 \leq a \leq 50$	8.54E-08	-1.00E-05	4.03E-04	-5.42E-03	<0.04
$50 \leq a \leq 60$	1.02E-06	-1.56E-04	8.01E-03	-1.37E-01	<0.42
$60 \leq a \leq 65$	1.41E-05	-2.52E-03	1.51E-01	-3.031	<0.023
For Hybrid (H1) Laminate					
$19 \leq a \leq 30$	5.06E-09	-2.56E-07	7.91E-06	-3.07E-05	<0.015
$30 \leq a \leq 40$	2.03E-08	-1.68E-06	5.23E-05	-4.95E-04	<0.03
$40 \leq a \leq 50$	1.14E-07	-1.33E-05	5.36E-04	-7.21E-03	<0.04
$50 \leq a \leq 60$	1.37E-06	-2.10E-04	1.08E-02	-1.85E-01	<0.42
$60 \leq a \leq 65$	1.89E-05	-3.39E-03	2.03E-01	-4.072	<0.023

For Hybrid (H2) Laminate					
$\mathbf{19 \leq a \leq 30}$	5.06E-09	-2.56E-07	7.91E-06	-3.07E-05	<0.015
$\mathbf{30 \leq a \leq 40}$	2.03E-08	-1.68E-06	5.23E-05	-4.95E-04	<0.03
$\mathbf{40 \leq a \leq 50}$	1.14E-07	-1.33E-05	5.36E-04	-7.208E-03	<0.04
$\mathbf{50 \leq a \leq 60}$	1.37E-06	-2.10E-04	1.08E-02	-1.85E-01	<0.42
$\mathbf{60 \leq a \leq 65}$	1.89E-05	-3.39E-03	2.033E-01	-4.072	<0.023

4.3. Critical Energy Release Rate (G_{IC}) Value

The critical energy release rate (G_{IC}) values for all composite laminates were evaluated using the load-displacement data (to get the experimental load as per ASTM E399) and with the formula mentioned in the data reduction method.

As presented in Table 11 and Figure 35 below, the fracture toughness value as per critical energy release rate value (G_{IC}) of Pure acacia tortilis laminate (AT) is very small, the G_{IC} value of Hybrid (H1) (G-AT-G-AT-G-AT-G) was higher than Hybrid (H2) (G-G-AT-AT-AT-G-G) as the presence of glass fiber orientation in the middle layer of the laminate sequence helped to resist the crack propagation more than Hybrid (H2). The G_{IC} value of pure glass laminate composite was found to be higher as expected, even though it was included in testing for comparison purposes. The G_{IC} value of Hybrid (H1) and Hybrid (H2) in between pure acacia tortilis composite laminate (AT) and pure glass laminate (G).

Table 11 critical energy release rate values for all composite laminates

Laminates	G_{IC} value ($\boldsymbol{kJ/m^2}$)	Standard dev. (SD) ($\boldsymbol{kJ/m^2}$)
Pure Acacia Tortilis Laminate (AT)	1.83	1.06
Hybrid (H1)	24.82	1.48
Hybrid (H2)	21.6	2.73
Pure Glass Laminate (G)	37.1	5.78

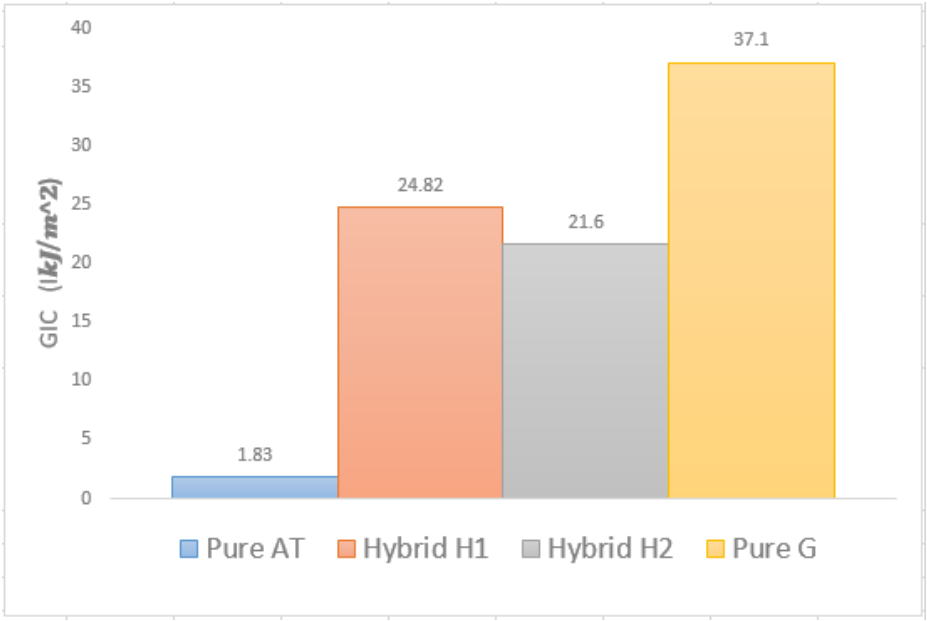

Figure 35 Critical energy release rate values for all composite laminates

For both of the hybrid laminates Hybrid (H1) and Hybrid (H2), 17% in %wt or 56.67% of glass fiber was added in pure acacia tortilis fiber composite laminate with different layer sequences.

By considering AT fiber composite laminate as a reference, 56.67% of glass fiber introduction into pure acacia tortilis fiber composite laminate results in an increase of critical energy release rate (G_{IC}) value by 92.62% for hybrid (H1), and 56.67% of glass fiber introduction into pure acacia tortilis fiber composite laminate results in an increase of critical energy release rate (G_{IC}) value by 91.52% for hybrid (H2).

By considering glass fiber composite laminate as a reference, 43.33% of AT fiber introduction in pure glass fiber composite laminate results in lowered critical energy release rate (G_{IC}) value of pure glass composite laminate by 41.78% for hybrid (H2), and 43.33% of AT fiber introduction in pure glass fiber composite laminate results in lowered critical energy release rate (G_{IC}) value of pure glass composite laminate by 33.09% for hybrid (H1).

The comparison for the intralaminar fracture toughness values using equation 3.10 in the data reduction method and using ASTM E399-09 testing standard[52] for metallic material along with the percentage difference is presented in Table 11.

Table 12 Intralaminar fracture toughness (based on G_{IC} value) comparison using ASTM E399-09 testing standard and using equation 3.10

Laminates	**Pure AT**	**Hybrid (H1)**	**Hybrid (H2)**	**Pure G**
G_{IC} (kJ/m^2), using eqn. 3.10	1.83	24.82	21.6	37.1
G_{IC} (kJ/m^2), using ASTM E399 standard	1.40	19.02	16.51	28.33
Difference (%)	23.49%	23.4%	23.56%	23.64%

From Table 12 above it is noted that the critical energy release rate value as per ASTM E399-09 standard is lowered by around 24% than the G_{IC} value computed using equation 3.10. This shows a significant difference between them and the use of the ASTM E399-09 standard for orthotropic composite materials is not recommended suchlike a difference between the values was also occurred in [45]. For comparison purposes, the intralaminar fracture toughness values along with the utilized data reduction method for some of the related composites were presented in Table 13. The G_{IC} value of pure AT was found to be smaller than that of sisal short fiber polymer composite, coconut short fiber polymer composite, and woven sisal polymer composite. The G_{IC} value of pure glass fiber composite is almost similar as in [75].

Table 13 Intralaminar fracture toughness values of some related polymer composites

Composite	**Fiber content and fiber type**	**G_{IC} (kJ/m^2)**	**Data reduction method**	**Ref.**
Sisal short fiber polymer composite	27% V_f	7	ASTM D5045	[60]
Coconut short fiber polymer composite	18% V_f	8	ASTM D5045	
Woven sisal polymer composite	30% V_f	11.3	ASTM D5045	
Chopped Sisal/Epoxy	30% wt%	13.72	ASTM D5045	[58]

composite				
Woven/chopped glass fiber hybrid polymer composite.	Random Chopped long fiber, fiber weight =30%	78.2	ASTM E399	[76]

4.4. Resistance Curve (R-Curve, G_{IC} Vs a)

The resistance curve was plotted using the recorded video during a test (used to note the crack propagation length at specific time), load-displacement data (used to read the load at that specific noted time for a specific propagated crack length 'a'), reduction technique (used to interpolate the polynomial coefficients 'C_i's and evaluate the value of G_{IC}). The R-curves for all composite laminates were presented in figure 36 (a)-(d).

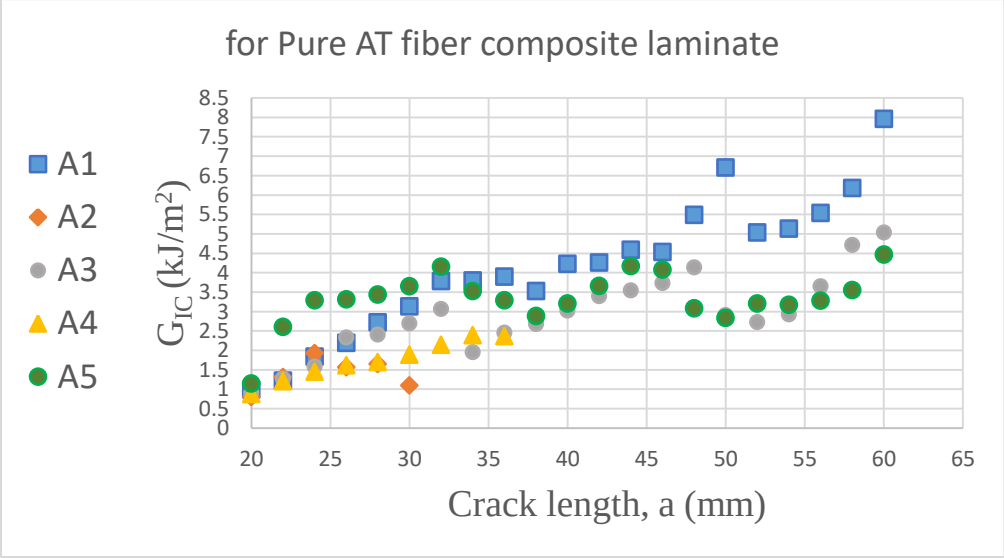

(a)

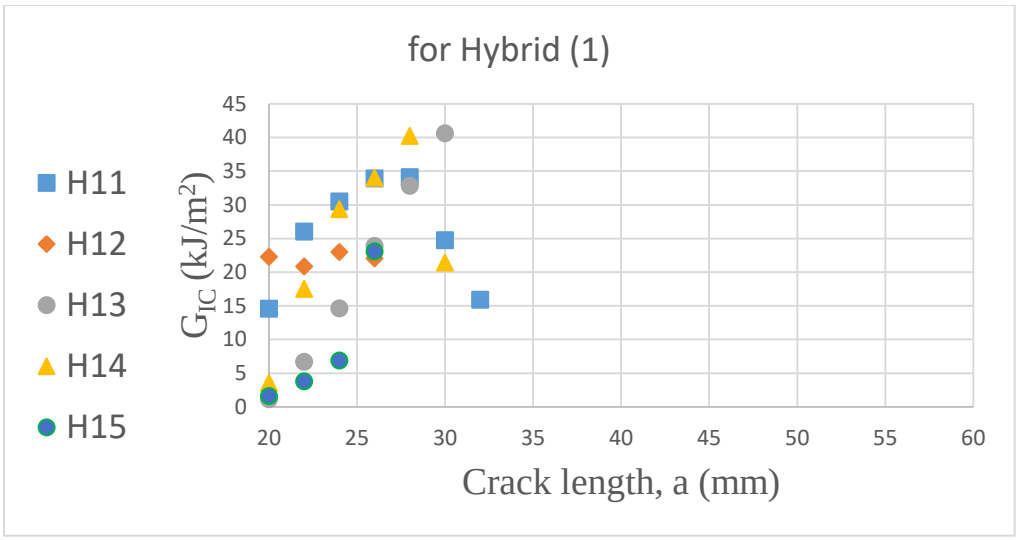
for Hybrid (1)
H11
H12
H13
H14
H15
G_{IC} (kJ/m^2)
Crack length, a (mm)

(b)

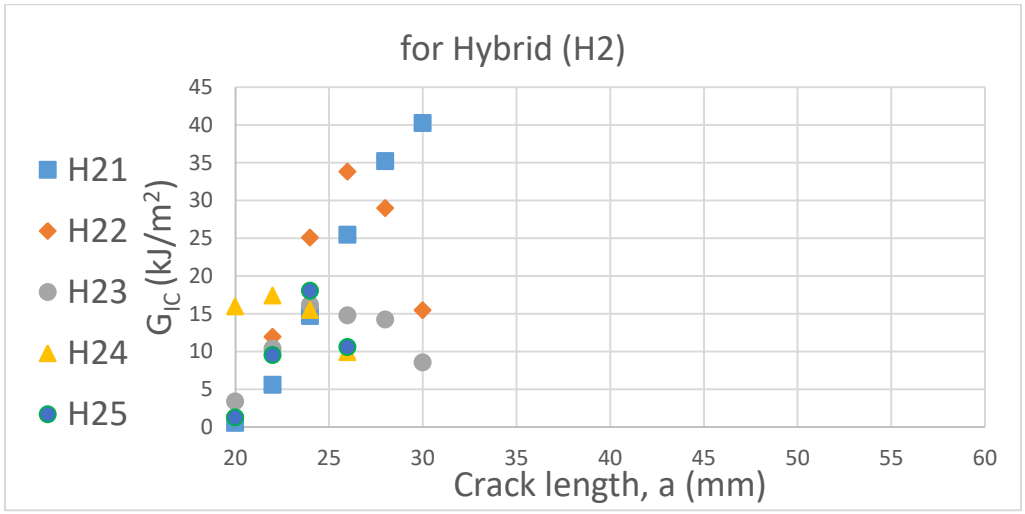
for Hybrid (H2)
H21
H22
H23
H24
H25
G_{IC} (kJ/m^2)
Crack length, a (mm)

(c)

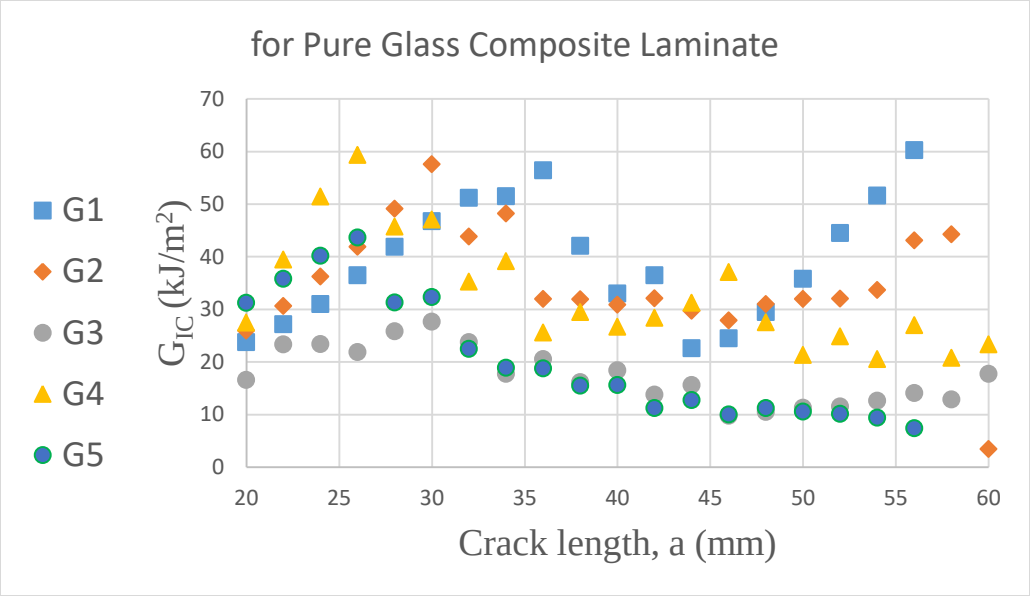

(d)

Figure 36 R- curve (a) for Pure AT fiber composite laminate, (b) for Hybrid (H1) (c) for Hybrid (H2), (c) for Pure Glass fiber composite laminate.

For pure AT, the resistance curves specimens 'A2' and 'A4' were plotted as their final propagated crack length only. The R-curve shows a high scattering pattern for a range of crack lengths up to 30mm which showed a positive trend. For a crack length of 30mm-40mm somehow less scattering (negative trend) was observed, for a crack length of 40mm to around 46mm again a higher scattering pattern and for the rest of the crack length, less scattering was observed. Generally, from the R-curve of the pure AT laminate, it can be understood that the R-curve behaves a positive trend for a crack length up to around 46mm and behaves a negative trend afterward by excluding the specimen 'A2', and 'A4'. Even though there was no visible damage other than crack propagation.

For hybrid (H1) and hybrid (H2), the resistance curves for all specimens of both hybrid laminates were plotted as their final propagated crack length only. And since there was unstable crack propagation for both hybrids, the time last for the total propagated crack length was evenly distributed in the resistance curve plotting procedure. From the R-curve result of both hybrid laminates less scattering was observed for a crack length up to 5mm which is a positive trend and a higher scattering for the rest of the range. The negative trend of R-curves for both hybrids composite laminates results from compressive failure such as delamination and matrix breakage.

For pure Glass, the R-curves pattern of all specimens of this composite laminate were almost similar throughout the crack length which showed appositive trend has been observed for the initial crack length up to 10 mm and for a crack length range from 35mm to 45mm & a negative trend for the rest of the range. Generally, the R-curve pattern of all composite laminates are in good comparable with the R-curve pattern in [45] [47].

4.5. Fractography

In order to qualitatively discuss the fractography of the specimens, a representative magnified front view of the fractured specimens for all composite laminates from the video recorded during-testing (Figure 37 (a)-(d)) and opened fracture surface of a representative specimens for all composite laminates (Figure 38 (a)-(d)) were presented.

(a)

(b)

(c)

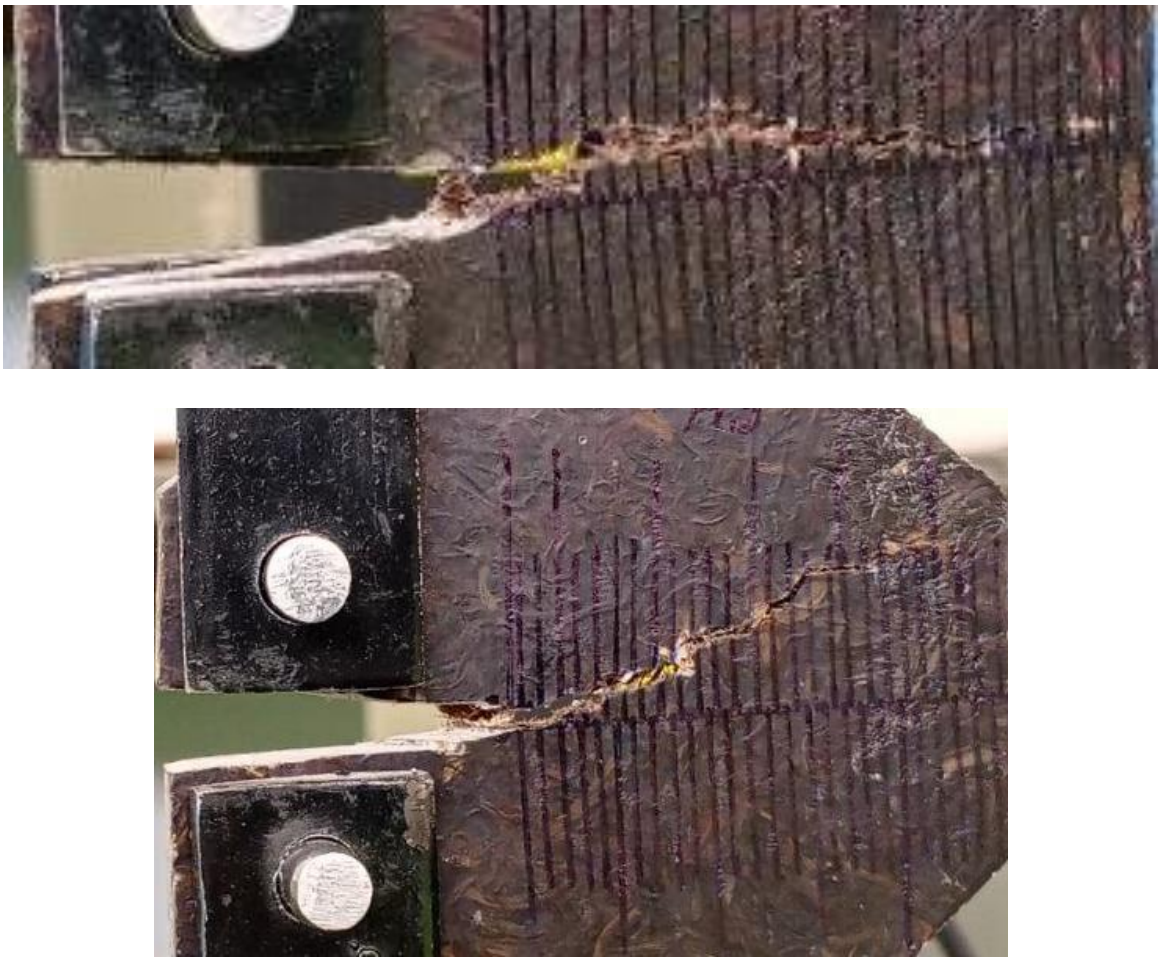

(d)

Figure 37 (a) close-up front view for pure Glass, (b) close-up front view for hybrid (H1), (c) close-up front view for hybrid (H2), (d) close-up front view for pure AT

For pure glass fiber composite laminate specimens, crack propagation was in the expected crack plane and damage other than crack propagation has not been seen. Crack propagation was smooth and progressive for all specimens of the composite laminates, a slight fiber pullout and tow splitting (break of fiber bundles) has been seen, and the direction of crack propagation was on the centerline and slightly above the center line. From the result, it has been seen that the fracture behavior of this composite laminate brittle fracture.

For hybrid (H1) and hybrid (H2) composite laminate specimens, initially the crack propagation was in the expected crack plane (straight forward up to some crack length) then it goes downward or upward in both forward directions. Unstable crack propagation has been seen for both hybrid specimens. For both hybrid laminates, a tow splitting has been seen on the outer

layer (glass) of the laminate and a delamination mode of failure was also recorded. The result showed that the fracture behavior was a brittle fracture.

For the above three laminates (pure G, hybrid (H1), hybrid (H2)), it has been seen a common and visible compressive failure such as fiber kinking, matrix breakage, and interlayer delamination. The interlayer delamination failure tells us there was a weak bonding between layers mainly for the hybrids.

For pure AT fiber composite laminate specimens, crack propagation was in the expected crack plane and damage other than crack propagation has not been seen. Crack propagation was smooth and progressive for all specimens of the composite laminates but it was faster than all the 3 laminates. Recorded direction of crack propagation was on slightly above the center line, initially through expected crack plane then propagated upward forward and downward forward. From the result it has been seen that the laminate behaves brittle fracture.

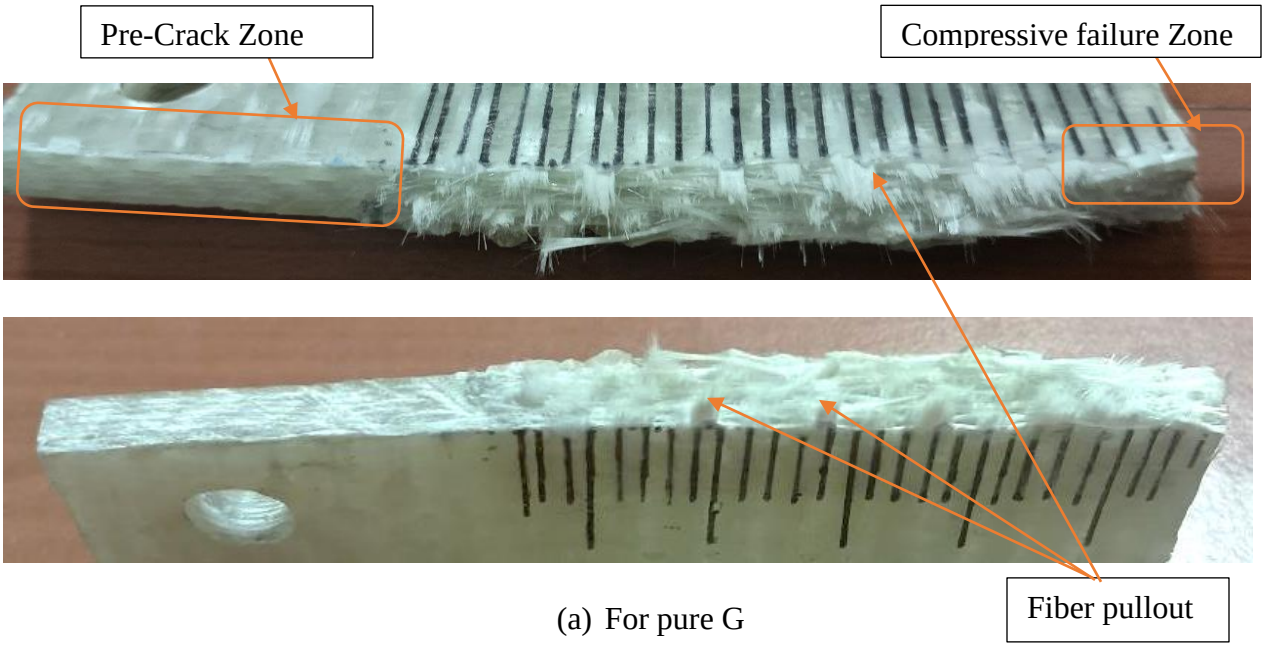

(a) For pure G

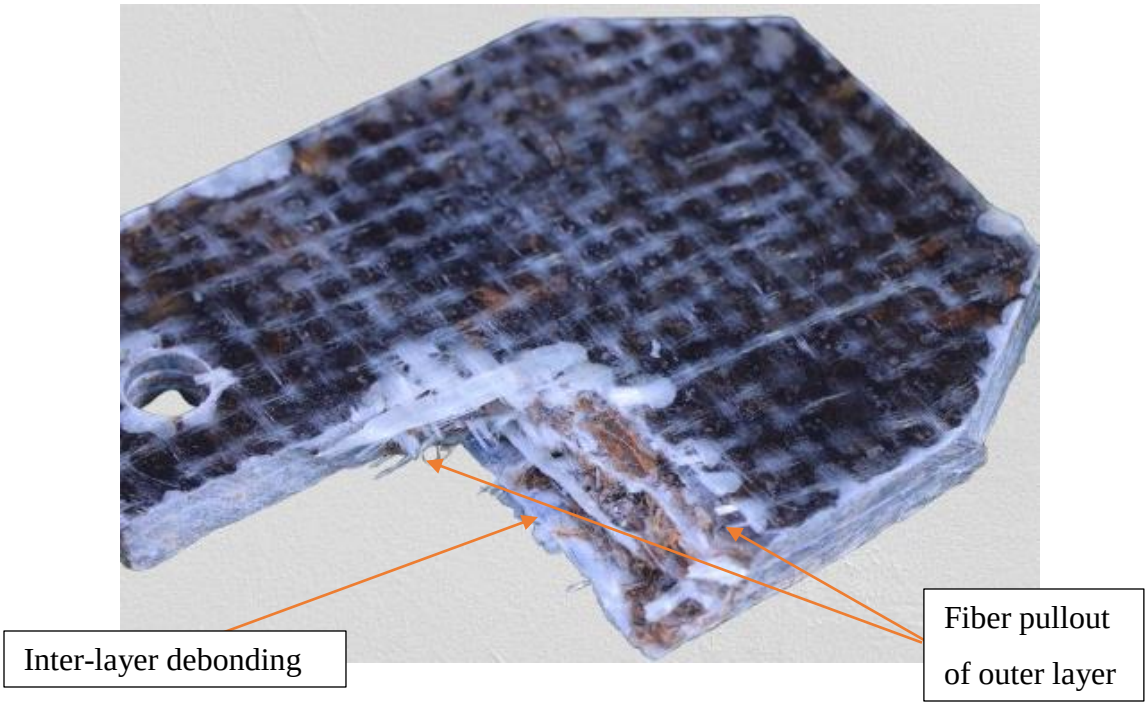

(b) For hybrid (H1)

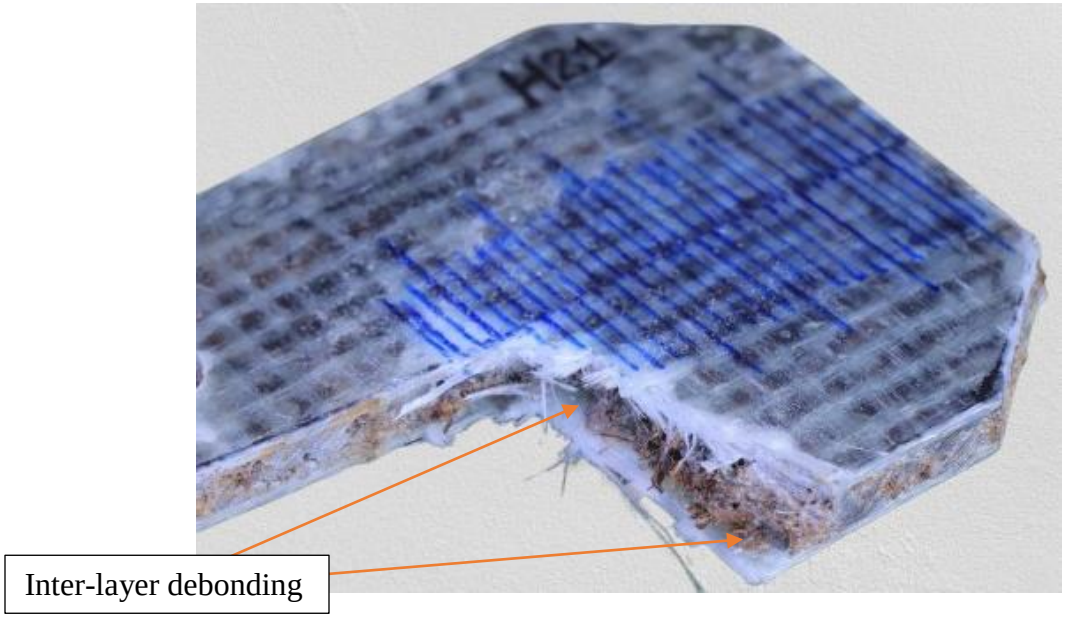

(c) For hybrid (H2)

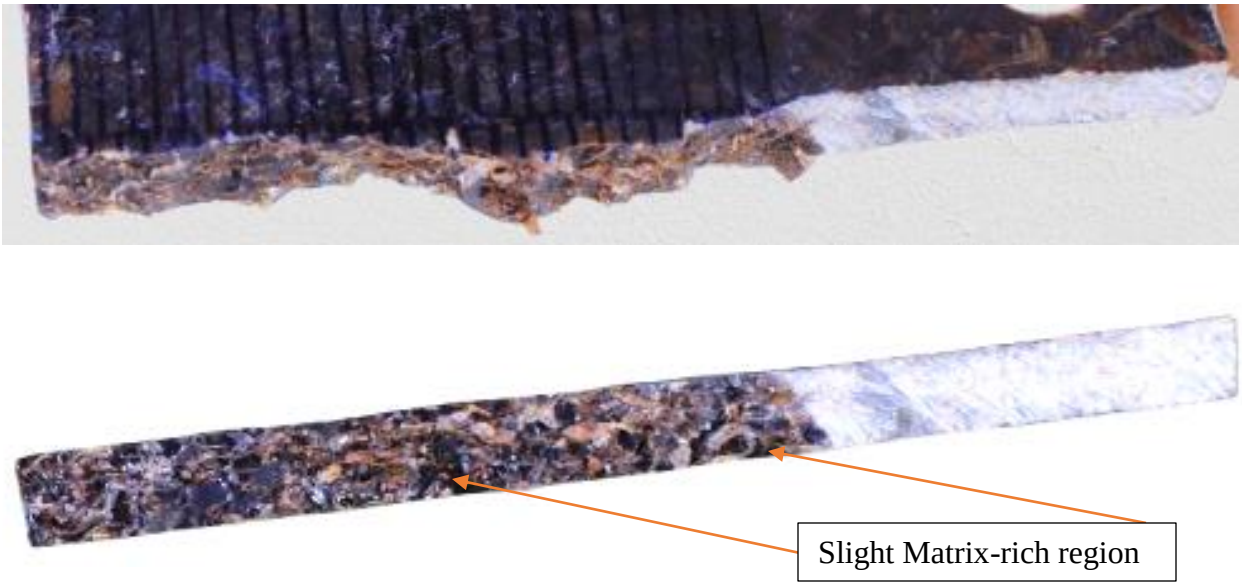

(d) For pure AT

Figure 38 opened fracture surface of a representative specimen (a) for pure G, (b) for hybrid (H1), (c) for hybrid (H2), (d) for pure AT

As shown in figure 38 (a)-(d) above, from the fractured surface of pure glass composite laminate, it was observed a fiber pullout, tow splitting in the crack propagation zone. In compressive failure zone on the right end side of the specimen, matrix breakage and slight delamination were observed. From the fracture surface of hybrid (H1) and hybrid (H2) it was observed a weak interlayer bonding, delamination, slight fiber pullout from the outer layer. From the fractured surface of pure acacia tortilis composite laminate, it was observed that the fiber-matrix uniformity was very interesting (as it was fabricated using hand lay-up method) except in the indicated location (figure 38d) at which propagates through matrix-rich region and back to the expected crack propagation plane.

5. Conclusion and Recommendations

5.1. Conclusion

In this study an experimental investigation on intralaminar fracture toughness of acacia tortilis/glass fiber reinforced polyester composite has been carried out. Pure AT fiber composite, hybrid (H1), hybrid (H2), and pure glass fiber composite laminates was prepared. From these four composite laminates five 2TCT (doubly tapered compact tension) specimens were prepared and have been tested. a data reduction technique along with FE analysis using Abaqus (CAE 2017) was employed. During the test, the crack propagation was observed in the expected plane for pure AT and pure glass fiber composite laminates (no other damages occurred), unstable crack propagation was observed for hybrid (H1) and hybrid (H2) laminates by searching weak zone of the laminate as the fiber is chopped and randomly oriented. Generally, from the result of crack propagation it can be concluded that the selected 2TCT specimen was favored for expected crack propagation.

From the load-displacement curves of the four composite laminates it was observed a similar behavior along all the phases starting from pre-loading to failure. The critical energy release rate (G_{IC}) value was computed using the load-displacement data along with data reduction technique. The G_{IC} value for pure AT, hybrid (H1), hybrid (H2), pure G laminates were found to be 1.83 kJ/m^2, 24.82 kJ/m^2, 21.6 kJ/m^2, 37.1 kJ/m^2 respectively. The G_{IC} value for pure AT was found to be very small and the hybridization of woven glass fiber for pure AT composite results an increase in G_{IC} value by 92.62% for hybrid (H1), and by 91.52% for hybrid (H2). The intralaminar fracture toughness values of the two hybrid composite laminates were in between pure AT and Pure G laminates. And the values are comparable with other natural fiber hybrid composites. The patterns of the R-curves for all composite laminates were with in common R-curve pattern trends. The fractoragraphy for all composite laminates were qualitatively described and discussed using digital camera images for fractured surfaces of the laminates. From the observation the fracture behavior for all laminates were brittle fracture and fiber pullout was observed for pure glass composite laminate, compressive failure was observed for pure G, hybrid (H1), and hybrid (H2).

5.2. Recommendations

From the results of study on all four composite laminates, it is recommended that the hybrid composite laminates can be a possible alternative for natural fiber/ glass fiber hybrid composite under a certain fracture toughness requirement for a specific application. The pure AT composite laminates is not recommended for a structural or non- structural application that needs a high and moderate fracture toughness value since the fracture toughness of the pure AT composite laminate was found very small.

It is possible to utilize the data reduction method and the 2TCT (doubly tapered compact tension specimen) recommended by Pinho et al. [47] in the previous literature and agreed by this study for the characterization of intralaminar fracture toughness of natural fiber polymer composite.

5.3. Further Future Works

In this research, an experimental investigation on intralaminar fracture toughness of acacia tortilis/ glass fiber reinforced polyester composite was studied by preparing four composite laminates (pure AT, hybrid (H1), hybrid (H2), and pure G). the research suggests and point out the following for further study.

- Investigation of interlaminar fracture toughness of AT/Glass fiber reinforced hybrid polymer composite.
- Characterization of the intralaminar fracture toughness of the composite under Mode-II, Mode-III, and mixed Mode loading condition.
- Experimental investigation on fiber orientation and fiber length effect on intralaminar fracture toughness of the composite.
- Investigation on the effect of different matrix materials as well as addition of Nano particles on the matrix.

References

[1] P. K. Mallick, *Fiber-Reinforced Composites: Materials, Manufacturing, and Design, Third Edition*, 0 ed. CRC Press, 2007. doi: 10.1201/9781420005981.

[2] K. Senthilkumar *et al.*, "Mechanical properties evaluation of sisal fibre reinforced polymer composites: A review," *Construction and Building Materials*, vol. 174, pp. 713–729, Jun. 2018, doi: 10.1016/j.conbuildmat.2018.04.143.

[3] A. V. Lima, J. L. Cardoso, and C. J. Lobo, "Research on hybrid sisal/glass composites: A review," *Journal of Reinforced Plastics and Composites*, vol. 38, no. 17, pp. 789–821, Sep. 2019, doi: 10.1177/0731684419847272.

[4] N. Venkateshwaran, A. Elayaperumal, and G. K. Sathiya, "Prediction of tensile properties of hybrid-natural fiber composites," *Composites Part B: Engineering*, vol. 43, no. 2, pp. 793–796, Mar. 2012, doi: 10.1016/j.compositesb.2011.08.023.

[5] X.-K. Zhu and J. A. Joyce, "Review of fracture toughness (G, K, J, CTOD, CTOA) testing and standardization," *Engineering Fracture Mechanics*, vol. 85, pp. 1–46, May 2012, doi: 10.1016/j.engfracmech.2012.02.001.

[6] J. B. Dawit, H. G. Lemu, and S. A. Tewelde, "Tensile and Flexural Properties of Acacia Tortilis/Glass Fiber Reinforced Hybrid Composites," in *Advanced Manufacturing and Automation XI*, Y. Wang, K. Martinsen, T. Yu, and K. Wang, Eds., in Lecture Notes in Electrical Engineering. Singapore: Springer, 2022, pp. 187–197. doi: 10.1007/978-981-19-0572-8_24.

[7] S. Jayabal, U. Natarajan, and S. Sathiyamurthy, "Effect of glass hybridization and staking sequence on mechanical behaviour of interply coir–glass hybrid laminate," *Bull Mater Sci*, vol. 34, no. 2, pp. 293–298, Apr. 2011, doi: 10.1007/s12034-011-0081-9.

[8] M. K. Egbo, "A fundamental review on composite materials and some of their applications in biomedical engineering," *Journal of King Saud University - Engineering Sciences*, vol. 33, no. 8, pp. 557–568, Dec. 2021, doi: 10.1016/j.jksues.2020.07.007.

[9] S. Bhati, S. Panwar, and S. Divya, "Composites and Its Applications: A Review," *SSRN Journal*, 2020, doi: 10.2139/ssrn.3904471.

[10] Y. Yang, R. Boom, B. Irion, D.-J. Van Heerden, P. Kuiper, and H. De Wit, "Recycling of composite materials," *Chemical Engineering and Processing: Process Intensification*, vol. 51, pp. 53–68, Jan. 2012, doi: 10.1016/j.cep.2011.09.007.

[11] R. Patwa and A. Telang, "Analysis of Cross-ply Laminate composite under UD load based on CLPT by Ansys APDL," vol. 5, no. 9, 2015.

[12] J. N. Reddy and J. N. Reddy, *Mechanics of laminated composite plates and shells: theory and analysis*, 2nd ed. Boca Raton: CRC Press, 2004.

[13] M. O. Kaman, "Effect of fiber orientation on fracture toughness of laminated composite plates [0°/θ°]s," *Engineering Fracture Mechanics*, vol. 78, no. 13, pp. 2521–2534, Aug. 2011, doi: 10.1016/j.engfracmech.2011.06.005.

[14] A. K. Kaw, *Mechanics of composite materials*, 2nd ed. Boca Raton, FL: Taylor & Francis, 2006.

[15] P. M. Manne and S. W. Tsai, "Practical Considerations for the Design of Composite Structures," *Mech. of Adv. Mat. & Structures*, vol. 5, no. 3, pp. 227–255, Jul. 1998, doi: 10.1080/10759419808945900.

[16] K. P. Ashik and R. S. Sharma, "A Review on Mechanical Properties of Natural Fiber Reinforced Hybrid Polymer Composites," *JMMCE*, vol. 03, no. 05, pp. 420–426, 2015, doi: 10.4236/jmmce.2015.35044.

[17] D. K. Rajak, P. H. Wagh, and E. Linul, “A Review on Synthetic Fibers for Polymer Matrix Composites: Performance, Failure Modes and Applications,” *Materials*, vol. 15, no. 14, p. 4790, Jul. 2022, doi: 10.3390/ma15144790.
[18] K. K. Chawla, *Composite materials: science and engineering*, 2nd ed. New York: Springer, 2011.
[19] N. Jauhari, R. Mishra, and H. Thakur, “Natural Fibre Reinforced Composite Laminates – A Review,” *Materials Today: Proceedings*, vol. 2, no. 4–5, pp. 2868–2877, 2015, doi: 10.1016/j.matpr.2015.07.304.
[20] J. B. Dawit, H. G. Lemu, Y. Regassa, and A. D. Akessa, “Investigation of the mechanical properties of Acacia tortilis fiber reinforced natural composite,” *Materials Today: Proceedings*, vol. 38, pp. 2953–2958, 2021, doi: 10.1016/j.matpr.2020.09.308.
[21] Y. Chen *et al.*, “Effect of fiber surface treatment on structure, moisture absorption and mechanical properties of luffa sponge fiber bundles,” *Industrial Crops and Products*, vol. 123, pp. 341–352, Nov. 2018, doi: 10.1016/j.indcrop.2018.06.079.
[22] X. Jiang, Y. Bai, X. Chen, and W. Liu, “A review on raw materials, commercial production and properties of lyocell fiber,” *Journal of Bioresources and Bioproducts*, vol. 5, no. 1, pp. 16–25, Feb. 2020, doi: 10.1016/j.jobab.2020.03.002.
[23] H. F. AbdElRahman and K. Krzywinski, “Environmental effects on morphology of Acacia tortilis group in the Red Sea Hills, North-Eastern Sudan and South-Eastern Egypt,” *Forest Ecology and Management*, vol. 255, no. 1, pp. 254–263, Feb. 2008, doi: 10.1016/j.foreco.2007.09.021.
[24] F. Abdallah, Z. Noumi, A. Ouled-Belgacem, R. Michalet, B. Touzard, and M. Chaieb, “The influence of Acacia tortilis (Forssk.) ssp. raddiana (Savi) Brenan presence, grazing, and water availability along the growing season, on the understory herbaceous vegetation in southern Tunisia,” *Journal of Arid Environments*, vol. 76, pp. 105–114, Jan. 2012, doi: 10.1016/j.jaridenv.2011.06.002.
[25] J. D. Deans *et al.*, “Comparative growth, biomass production, nutrient use and soil amelioration by nitrogen-fixing tree species in semi-arid Senegal,” *Forest Ecology and Management*, vol. 176, no. 1–3, pp. 253–264, Mar. 2003, doi: 10.1016/S0378-1127(02)00296-7.
[26] A. Gebrekirstos, D. Teketay, M. Fetene, and R. Mitlöhner, “Adaptation of five co-occurring tree and shrub species to water stress and its implication in restoration of degraded lands,” *Forest Ecology and Management*, vol. 229, no. 1–3, pp. 259–267, Jul. 2006, doi: 10.1016/j.foreco.2006.04.029.
[27] S. Tefera, H. A. Snyman, and G. N. Smit, “Rangeland dynamics of southern Ethiopia: (2). Assessment of woody vegetation structure in relation to land use and distance from water in semi-arid Borana rangelands,” *Journal of Environmental Management*, vol. 85, no. 2, pp. 443–452, Oct. 2007, doi: 10.1016/j.jenvman.2006.10.008.
[28] P. Alam *et al.*, “Comparative study of antioxidant activity and validated RP-HPTLC analysis of rutin in the leaves of different Acacia species grown in Saudi Arabia,” *Saudi Pharmaceutical Journal*, vol. 25, no. 5, pp. 715–723, Jul. 2017, doi: 10.1016/j.jsps.2016.10.010.
[29] S. Gabr *et al.*, “Characterization and optimization of phenolics extracts from Acacia species in relevance to their anti-inflammatory activity,” *Biochemical Systematics and Ecology*, vol. 78, pp. 21–30, Jun. 2018, doi: 10.1016/j.bse.2018.03.001.

[30] E. V. M. Kigondu *et al.*, “Anti-parasitic activity and cytotoxicity of selected medicinal plants from Kenya,” *Journal of Ethnopharmacology*, vol. 123, no. 3, pp. 504–509, Jun. 2009, doi: 10.1016/j.jep.2009.02.008.
[31] A. K. Lakhera and V. Kumar, “Monosaccharide composition of acidic gum exudates from Indian Acacia tortilis ssp. raddiana (Savi) Brenan,” *International Journal of Biological Macromolecules*, vol. 94, pp. 45–50, Jan. 2017, doi: 10.1016/j.ijbiomac.2016.09.097.
[32] J. B. Dawit, Y. Regassa, and H. G. Lemu, “Property characterization of acacia tortilis for natural fiber reinforced polymer composite,” *Results in Materials*, vol. 5, p. 100054, Mar. 2020, doi: 10.1016/j.rinma.2019.100054.
[33] D. Rajak, D. Pagar, P. Menezes, and E. Linul, “Fiber-Reinforced Polymer Composites: Manufacturing, Properties, and Applications,” *Polymers*, vol. 11, no. 10, p. 1667, Oct. 2019, doi: 10.3390/polym11101667.
[34] B. Middleton, “Composites: Manufacture and Application,” in *Design and Manufacture of Plastic Components for Multifunctionality*, Elsevier, 2016, pp. 53–101. doi: 10.1016/B978-0-323-34061-8.00003-X.
[35] Y. Zhou, M. Fan, and L. Chen, “Interface and bonding mechanisms of plant fibre composites: An overview,” *Composites Part B: Engineering*, vol. 101, pp. 31–45, Sep. 2016, doi: 10.1016/j.compositesb.2016.06.055.
[36] K. J. Wong, B. F. Yousif, and K. O. Low, “The effects of alkali treatment on the interfacial adhesion of bamboo fibres,” *Proceedings of the Institution of Mechanical Engineers, Part L: Journal of Materials: Design and Applications*, vol. 224, no. 3, pp. 139–148, Jul. 2010, doi: 10.1243/14644207JMDA304.
[37] C. Martínez Suárez, P. Rojas Montejo, and O. Gutiérrez Junco, “Effects of alkaline treatments on natural fibers,” *J. Phys.: Conf. Ser.*, vol. 2046, no. 1, p. 012056, Oct. 2021, doi: 10.1088/1742-6596/2046/1/012056.
[38] L. F. Ng, “Miscellaneous Study on Epoxy/Synthetic/Natural Fiber Hybrid Composites,” in *Handbook of Epoxy/Fiber Composites*, S. Mavinkere Rangappa, J. Parameswaranpillai, S. Siengchin, and S. Thomas, Eds., Singapore: Springer Nature Singapore, 2022, pp. 1029–1057. doi: 10.1007/978-981-19-3603-6_41.
[39] S. O. Ismail, E. Akpan, and H. N. Dhakal, “Review on natural plant fibres and their hybrid composites for structural applications: Recent trends and future perspectives,” *Composites Part C: Open Access*, vol. 9, p. 100322, Oct. 2022, doi: 10.1016/j.jcomc.2022.100322.
[40] M. Ö. Seydibeyoğlu *et al.*, “Review on Hybrid Reinforced Polymer Matrix Composites with Nanocellulose, Nanomaterials, and Other Fibers,” *Polymers*, vol. 15, no. 4, p. 984, Feb. 2023, doi: 10.3390/polym15040984.
[41] E. M. Araújo, K. D. Araújo, O. D. Pereira, P. C. Ribeiro, and T. J. A. D. Melo, “Fiberglass wastes/polyester resin composites: mechanical properties and water sorption,” *Polímeros*, vol. 16, no. 4, pp. 332–335, Dec. 2006, doi: 10.1590/S0104-14282006000400014.
[42] M. Ashokkumar and S. Supriya, “Fracture Toughness Evaluation of Particle Filled Composite,” vol. 5, no. 9, 2018.
[43] R. Talreja, “A mechanisms-based framework for describing failure in composite materials,” in *Structural Integrity and Durability of Advanced Composites*, Elsevier, 2015, pp. 25–42. doi: 10.1016/B978-0-08-100137-0.00002-X.
[44] M. J. Laffan, S. T. Pinho, P. Robinson, and A. J. McMillan, “Translaminar fracture toughness testing of composites: A review,” *Polymer Testing*, vol. 31, no. 3, pp. 481–489, May 2012, doi: 10.1016/j.polymertesting.2012.01.002.

[45] S. T. Pinho, P. Robinson, and L. Iannucci, “Fracture toughness of the tensile and compressive fibre failure modes in laminated composites,” *Composites Science and Technology*, vol. 66, no. 13, pp. 2069–2079, Oct. 2006, doi: 10.1016/j.compscitech.2005.12.023.
[46] M. F. S. F. De Moura, R. D. S. G. Campilho, A. M. Amaro, and P. N. B. Reis, “Interlaminar and intralaminar fracture characterization of composites under mode I loading,” *Composite Structures*, vol. 92, no. 1, pp. 144–149, Jan. 2010, doi: 10.1016/j.compstruct.2009.07.012.
[47] N. Blanco, D. Trias, S. T. Pinho, and P. Robinson, “Intralaminar fracture toughness characterisation of woven composite laminates. Part II: Experimental characterisation,” *Engineering Fracture Mechanics*, vol. 131, pp. 361–370, Nov. 2014, doi: 10.1016/j.engfracmech.2014.08.011.
[48] M. W. Czabaj and J. G. Ratcliffe, “Comparison of intralaminar and interlaminar mode I fracture toughnesses of a unidirectional IM7/8552 carbon/epoxy composite,” *Composites Science and Technology*, vol. 89, pp. 15–23, Dec. 2013, doi: 10.1016/j.compscitech.2013.09.008.
[49] M. S. S. Prasad, C. S. Venkatesha, and T. Jayaraju, “Experimental Methods of Determining Fracture Toughness of Fiber Reinforced Polymer Composites under Various Loading Conditions,” *JMMCE*, vol. 10, no. 13, pp. 1263–1275, 2011, doi: 10.4236/jmmce.2011.1013099.
[50] J. M. Barsom and S. T. Rolfe, *Fracture and fatigue control in structures: applications of fracture mechanics*, 3rd ed. West Conshohocken, PA: ASTM, 1999.
[51] H. R. Nejati, A. Nazerigivi, M. Imani, and A. Karrech, “Monitoring of fracture propagation in brittle materials using acoustic emission techniques-A review,” *Computers and Concrete*, vol. 25, no. 1, pp. 15–27, Jan. 2020, doi: 10.12989/CAC.2020.25.1.015.
[52] E08 Committee, *Test Method for Linear-Elastic Plane-Strain Fracture Toughness KIc of Metallic Materials*. doi: 10.1520/E0399-09E02.
[53] D20 Committee, *Test Methods for Plane-Strain Fracture Toughness and Strain Energy Release Rate of Plastic Materials*. doi: 10.1520/D5045-14.
[54] D30 Committee, *Test Method for Translaminar Fracture Toughness of Laminated and Pultruded Polymer Matrix Composite Materials*. doi: 10.1520/E1922-04R15.
[55] N. Blanco, D. Trias, S. T. Pinho, and P. Robinson, “Intralaminar fracture toughness characterisation of woven composite laminates. Part I: Design and analysis of a compact tension (CT) specimen,” *Engineering Fracture Mechanics*, vol. 131, pp. 349–360, Nov. 2014, doi: 10.1016/j.engfracmech.2014.08.012.
[56] R. F. Pinto, G. Catalanotti, and P. P. Camanho, “Measuring the intralaminar crack resistance curve of fibre reinforced composites at extreme temperatures,” *Composites Part A: Applied Science and Manufacturing*, vol. 91, pp. 145–155, Dec. 2016, doi: 10.1016/j.compositesa.2016.10.004.
[57] C. Zhao *et al.*, “Intralaminar crack propagation of glass fiber reinforced composite laminate,” *Structures*, vol. 41, pp. 787–803, Jul. 2022, doi: 10.1016/j.istruc.2022.05.064.
[58] A. Abera Betelie, Y. Tsegaye Megera, D. Telahun Redda, A. Sinclair, and School of Mechanical and Industrial Engineering, Addis Ababa University, AAiT King George VI Street-385, Addis Ababa, Ethiopia, “Experimental investigation of fracture toughness for treated sisal epoxy composite,” *AIMS Materials Science*, vol. 5, no. 1, pp. 93–104, 2018, doi: 10.3934/matersci.2018.1.93.

[59] M. Hughes, C. A. S. Hill, and J. R. B. Hague, “[The fracture toughness of bast fibre reinforced polyester composites Part 1 Evaluation and analysis],” *Journal of Materials Science*, vol. 37, no. 21, pp. 4669–4676, 2002, doi: 10.1023/A:1020621020862.
[60] R. V. Silva, D. Spinelli, W. W. Bose Filho, S. Claro Neto, G. O. Chierice, and J. R. Tarpani, “Fracture toughness of natural fibers/castor oil polyurethane composites,” *Composites Science and Technology*, vol. 66, no. 10, pp. 1328–1335, Aug. 2006, doi: 10.1016/j.compscitech.2005.10.012.
[61] Y. Zhang, Y. Li, H. Ma, and T. Yu, “Tensile and interfacial properties of unidirectional flax/glass fiber reinforced hybrid composites,” *Composites Science and Technology*, vol. 88, pp. 172–177, Nov. 2013, doi: 10.1016/j.compscitech.2013.08.037.
[62] P. S. S. Gouda, S. K. Kudari, S. Prabhuswamy, and D. Jawali, “Fracture Toughness of Glass-Carbon (0/90)_s Fiber Reinforced Polymer Composite – An Experimental and Numerical Study,” *JMMCE*, vol. 10, no. 08, pp. 671–682, 2011, doi: 10.4236/jmmce.2011.108052.
[63] M. V. Donadon, B. G. Falzon, L. Iannucci, and J. M. Hodgkinson, “Intralaminar toughness characterisation of unbalanced hybrid plain weave laminates,” *Composites Part A: Applied Science and Manufacturing*, vol. 38, no. 6, pp. 1597–1611, Jun. 2007, doi: 10.1016/j.compositesa.2006.12.003.
[64] P. K. Naik, N. V. Londe, B. Yogesha, L. Laxmana Naik, and K. V. Pradeep, “Mode I Fracture Characterization of Banana Fibre Reinforced Polymer Composite,” *IOP Conf. Ser.: Mater. Sci. Eng.*, vol. 376, p. 012041, Jun. 2018, doi: 10.1088/1757-899X/376/1/012041.
[65] P. K. Mallick, *Fiber-reinforced composites: materials, manufacturing, and design*, 3. ed. Boca Raton, Fla.: CRC Press, 2008.
[66] S. Rana and R. Fangueiro, Eds., *Advanced composite materials for aerospace engineering: processing, properties and applications*. in Woodhead Publishing series in composites science and engineering, no. Number 70. Amsterdam: Elsevier/Woodhead Publishing, 2016.
[67] F. Sarasini and V. Fiore, “A systematic literature review on less common natural fibres and their biocomposites,” *Journal of Cleaner Production*, vol. 195, pp. 240–267, Sep. 2018, doi: 10.1016/j.jclepro.2018.05.197.
[68] A. Q. Dayo *et al.*, “The influence of different chemical treatments on the hemp fiber/polybenzoxazine based green composites: Mechanical, thermal and water absorption properties,” *Materials Chemistry and Physics*, vol. 217, pp. 270–277, Sep. 2018, doi: 10.1016/j.matchemphys.2018.06.040.
[69] P. Zuo, D. V. Srinivasan, and A. P. Vassilopoulos, “Review of hybrid composites fatigue,” *Composite Structures*, vol. 274, p. 114358, Oct. 2021, doi: 10.1016/j.compstruct.2021.114358.
[70] A. Khoramshahi and N. Choupani, “Influence of Mixed-Mode Ratio on Delamination Fracture Toughness and Energy Release Rate of Glass/Polyester Laminates,” *KEM*, vol. 471–472, pp. 874–879, Feb. 2011, doi: 10.4028/www.scientific.net/KEM.471-472.874.
[71] H. Herranen *et al.*, “Design and Testing of Sandwich Structures with Different Core Materials,” *ms*, vol. 18, no. 1, pp. 45–50, Mar. 2012, doi: 10.5755/j01.ms.18.1.1340.
[72] T. Sathishkumar, S. Satheeshkumar, and J. Naveen, “Glass fiber-reinforced polymer composites – a review,” *Journal of Reinforced Plastics and Composites*, vol. 33, no. 13, pp. 1258–1275, Jul. 2014, doi: 10.1177/0731684414530790.

[73] R. M. Jones, *Mechanics of Composite Materials*, 2nd ed. CRC Press, 2018. doi: 10.1201/9781498711067.
[74] G. Pappas, L. P. Canal, and J. Botsis, "Characterization of intralaminar mode I fracture of AS4/PPS composite using inverse identification and micromechanics," *Composites Part A: Applied Science and Manufacturing*, vol. 91, pp. 117–126, Dec. 2016, doi: 10.1016/j.compositesa.2016.09.018.
[75] D. S. Rao, P. R. Reddy, and S. Venkatesh, "Determination of Mode-I Fracture Toughness of Epoxy-Glass Fibre Composite Laminate," *Procedia Engineering*, vol. 173, pp. 1678–1683, 2017, doi: 10.1016/j.proeng.2016.12.193.
[76] A. O. Ozdemir and C. Karatas, "Experimental Determination of Fracture Toughness of Woven/Chopped Glass Fiber Hybrid Reinforced Thermoplastic Composite Laminates," *Scientia Iranica*, vol. 0, no. 0, pp. 0–0, Dec. 2020, doi: 10.24200/sci.2020.56380.4701.

Appendixes

Appendix A: Calculation on mass-volume content of Fiber and Matrix of the Composite

Laminate 1-Pure Glass: G/G/G/G/G/G/G

- **Constant parameters**
  - $Total\ volume\ fraction\ v_f = \mathbf{0.3}$
  - $Required\ AT\ fiber\ v_{AT} = \mathbf{0}$
  - $Required\ Glass\ fiber\ v_G = \mathbf{0.3}$
  - $Required\ relative\ AT\ fiber: Glass\ fiber = \mathbf{0}$
  - $Density\ of\ AT\ fiber, \rho_{AT}\ (g/cm^3) = \mathbf{0.906\ g/cm^3}$
  - $Density\ of\ glass\ fiber, \rho_G\ (g/cm^3) = \mathbf{2.54\ g/cm^3}$
  - $Density\ of\ polyester\ resin, \rho_{poly}\ (g/cm^3) = \mathbf{1.2 g/cm^3}$
  - $Volume\ of\ composite, V_C(cm^3) = (250mm * 200mm * 5.6mm) = \mathbf{280 cm^3}$
- **Calculated Parameters**
  - $Density\ of\ composite, \rho(g/cm\text{^}3)$

    $$\rho = \rho_f v_f + \rho_m v_m = (2.54\ g/cm^3 * 0.3) + (1.2 g/cm^3 * 0.7) = 0.762 + 0.84$$
    $$= \mathbf{1.602 g/cm^3}$$
  - $Mass\ of\ composite, m(g)$

    $$m = \rho_c * V_c = 1.602 g/cm^3 * 280 cm^3 = \mathbf{448.56 g}$$
  - $Volume\ of\ AT\ fiber\ (cm^3) = \mathbf{0}$
  - $Volume\ of\ glass\ fiber\ (cm^3)$

    $$V_g = v_g * V_c = 0.3 * 280 cm^3 = \mathbf{84 cm^3}$$
  - $Volume\ of\ polyester, V_{poly} = v_m * V_c = 0.7 * 280 cm^3 = \mathbf{196 cm^3}$
  - $Mass\ of\ AT\ fiber, m_{AT} = \mathbf{0}$
  - $Mass\ of\ glass\ fiber, m_g = \rho_g * V_g = 2.54 g/cm^3 * 84 cm^3 = \mathbf{213.36 g}$
  - $Mass\ of\ polyester, m_{poly} = m_c - m_g = 448.56 g - 213.36 g = \mathbf{235.2 g}$
  - $AT\ fiber\ wt\% = \mathbf{0}$
  - $Glass\ fiber\ wt\% = \frac{m_g}{m_c} = 213.56 g/448.56 g = \mathbf{0.4757}$
  - $Relative\ AT: G\ fiber\ wt\% = \mathbf{0}$

Laminate 2-Pure Acacia Tortilis: AT/AT/AT/AT/AT/AT/AT

- **Constant parameters**
  - $Total\ volume\ fraction\ v_f = \mathbf{0.3}$
  - $Required\ AT\ fiber\ v_{AT} = \mathbf{0.3}$
  - $Required\ Glass\ fiber\ v_G = \mathbf{0}$
  - $Required\ relative\ AT\ fiber: Glass\ fiber = \mathbf{1}$
  - $Density\ of\ AT\ fiber, \rho_{AT}\ (g/cm^3) = \mathbf{0.906\ g/cm^3}$
  - $Density\ of\ glass\ fiber, \rho_G\ (g/cm^3) = \mathbf{2.54\ g/cm^3}$
  - $Density\ of\ polyester\ resin, \rho_{poly}\ (g/cm^3) = \mathbf{1.2 g/cm^3}$
  - $Volume\ of\ composite, V_C(cm^3) = (250mm * 200mm * 5.6mm) = \mathbf{280 cm^3}$
- **Calculated Parameters**
  - $Density\ of\ composite, \rho(g/cm\text{^}3)$

    $\rho = \rho_f v_f + \rho_m v_m = (0.906\ g/cm^3 * 0.3) + (1.2 g/cm^3 * 0.7) = \mathbf{1.112 g/cm^3}$
  - $Mass\ of\ composite, m(g)$

    $$m = \rho_c * V_c = 1.112 g/cm^3 * 280 cm^3 = \mathbf{311.304 g}$$

    $$Volume\ of\ AT\ fiber\ (cm^3) = V_{AT} = v_{AT} * V_c = 0.3 * 280 cm^3 = \mathbf{84 cm^3}$$
  - $Volume\ of\ glass\ fiber\ (cm^3) = \mathbf{0}$
  - $Volume\ of\ polyester, V_{poly} = v_m * V_c = 0.7 * 280 cm^3 = \mathbf{196 cm^3}$
  - $Mass\ of\ AT\ fiber, m_{AT} = m_{AT} = \rho_{AT} * V_{AT} = 0.906 g/cm^3 * 84 cm^3 = \mathbf{76.104 g}$
  - $Mass\ of\ glass\ fiber, m_g = \mathbf{0}$
  - $Mass\ of\ polyester, m_{poly} = m_c - m_g = \rho_{poly} * V_{poly} = 1.2 g/cm^3 * 196 cm^3 = \mathbf{235.2 g}$
  - $AT\ fiber\ wt\% = \frac{m_{AT}}{m_C} = \frac{76.104 g}{311.304 g} = \mathbf{0.2445}$
  - $Glass\ fiber\ wt\% = \frac{m_g}{m_c} = \mathbf{0}$
  - $Relative\ AT: G\ fiber\ wt\% = \mathbf{1}$

Laminate 3-Hybrid (H1): G/AT/G/AT/G/AT/G

- **Constant parameters**
  - $Total\ volume\ fraction\ v_f = \mathbf{0.3}$
  - $Required\ AT\ fiber\ v_{AT} = \mathbf{0.13}$
  - $Required\ Glass\ fiber\ v_G = \mathbf{0.17}$
  - $Required\ relative\ AT\ fiber: Glass\ fiber = \mathbf{0.4333}$
  - $Density\ of\ AT\ fiber, \rho_{AT}\ (g/cm^3) = \mathbf{0.906\ g/cm^3}$
  - $Density\ of\ glass\ fiber, \rho_G\ (g/cm^3) = \mathbf{2.54\ g/cm^3}$
  - $Density\ of\ polyester\ resin, \rho_{poly}\ (g/cm^3) = \mathbf{1.2g/cm^3}$
  - $Volume\ of\ composite, V_C(cm^3) = (250mm * 200mm * 5.6mm) = \mathbf{280cm^3}$
- **Calculated Parameters**
  - $Density\ of\ composite, \rho(g/cm\text{^}3)$

    $\rho = \rho_f v_f + \rho_m v_m$

    $= (0.906g/cm^3 * 0.13) + (2.54\ g/cm^3 * 0.17) + (1.2g/cm^3 * 0.7)$

    $= \mathbf{1.3896g/cm^3}$
  - $Mass\ of\ composite, m(g)$

    $m = \rho_c * V_c = 1.3896g/cm^3 * 280cm^3 = \mathbf{389.088g}$
  - $Volume\ of\ AT\ fiber\ (cm^3) = v_{AT} * V_c = 0.13 * 280cm^3 = \mathbf{36.4cm^3}$
  - $Volume\ of\ glass\ fiber\ (cm^3)$

    $V_g = v_g * V_c = 0.17 * 280cm^3 = \mathbf{47.6cm^3}$
  - $Volume\ of\ polyester, V_{poly} = v_m * V_c = 0.7 * 280cm^3 = \mathbf{196cm^3}$
  - $Mass\ of\ AT\ fiber, m_{AT} = \rho_{AT} * V_{AT} = 0.906g/cm^3 * 36.4cm^3 = \mathbf{32.9784g}$
  - $Mass\ of\ glass\ fiber, m_g = \rho_g * V_g = 2.54\ g/cm^3 * 47.6cm^3 = \mathbf{120.904g}$
  - $Mass\ of\ polyester, m_{poly} = m_c - m_g = \rho_{poly} * V_{poly} = 1.2g/cm^3 * 196cm^3 = \mathbf{235.2g}$
  - $AT\ fiber\ wt\% = \mathbf{0.08475}$
  - $Glass\ fiber\ wt\% = \frac{m_g}{m_c} = \mathbf{0.3107}$
  - $Relative\ AT: G\ fiber\ wt\% = \mathbf{0.2143}$

Laminate 4-Hybrid (H2): G/G/AT/AT/AT/G/G

- **Constant parameters**
  - $Total\ volume\ fraction\ v_f = \mathbf{0.3}$
  - $Required\ AT\ fiber\ v_{AT} = \mathbf{0.13}$
  - $Required\ Glass\ fiber\ v_G = \mathbf{0.17}$
  - $Required\ relative\ AT\ fiber: Glass\ fiber = \mathbf{0.4333}$
  - $Density\ of\ AT\ fiber, \rho_{AT}\ (g/cm^3) = \mathbf{0.906\ g/cm^3}$
  - $Density\ of\ glass\ fiber, \rho_G\ (g/cm^3) = \mathbf{2.54\ g/cm^3}$
  - $Density\ of\ polyester\ resin, \rho_{poly}\ (g/cm^3) = \mathbf{1.2g/cm^3}$
  - $Volume\ of\ composite, V_C(cm^3) = (250mm * 200mm * 5.6mm) = \mathbf{280cm^3}$
- **Calculated Parameters**
  - $Density\ of\ composite, \rho(g/cm\text{^}3)$

    $\rho = \rho_f v_f + \rho_m v_m$

    $= (0.906g/cm^3 * 0.13) + (2.54\ g/cm^3 * 0.17) + (1.2g/cm^3 * 0.7)$

    $= \mathbf{1.3896g/cm^3}$
  - $Mass\ of\ composite, m(g)$

    $m = \rho_c * V_c = 1.3896g/cm^3 * 280cm^3 = \mathbf{389.088g}$
  - $Volume\ of\ AT\ fiber\ (cm^3) = v_{AT} * V_c = 0.13 * 280cm^3 = \mathbf{36.4cm^3}$
  - $Volume\ of\ glass\ fiber\ (cm^3)$

    $V_g = v_g * V_c = 0.17 * 280cm^3 = \mathbf{47.6cm^3}$
  - $Volume\ of\ polyester, V_{poly} = v_m * V_c = 0.7 * 280cm^3 = \mathbf{196cm^3}$
  - $Mass\ of\ AT\ fiber, m_{AT} = \rho_{AT} * V_{AT} = 0.906g/cm^3 * 36.4cm^3 = \mathbf{32.9784g}$
  - $Mass\ of\ glass\ fiber, m_g = \rho_g * V_g = 2.54\ g/cm^3 * 47.6cm^3 = \mathbf{120.904g}$
  - $Mass\ of\ polyester, m_{poly} = m_c - m_g = \rho_{poly} * V_{poly} = 1.2g/cm^3 * 196cm^3 = \mathbf{235.2g}$
  - $AT\ fiber\ wt\% = \mathbf{0.08475}$
  - $Glass\ fiber\ wt\% = \frac{m_g}{m_c} = \mathbf{0.3107}$
  - $Relative\ AT: G\ fiber\ wt\% = \mathbf{0.2143}$

Appendix B: *The normalized energy release rate* $f(a)$ (m^2/kJ) *for a crack length of a ranging from* $19mm - 64mm$ *as indicated by Blanco et al.* (2014).

For Laminate 1-Pure Acacia Tortilis fiber reinforced composite									
Crack length, a (mm)	19	20	21	22	23	24	25	26	27
f(a)	1.1306E-04	1.2027E-04	1.2766E-04	1.3533E-04	1.4325E-04	1.5151E-04	1.6014E-04	1.6922E-04	1.7879E-04
a	28	29	30	31	32	33	34	35	36
f(a)	1.8894E-04	1.9974E-04	2.1129E-04	2.2368E-04	2.3701E-04	2.5146E-04	2.6715E-04	2.8425E-04	3.0300E-04
a	37	38	39	40	41	42	43	44	45
f(a)	3.2351E-04	3.4628E-04	3.7151E-04	3.9946E-04	4.3072E-04	4.6578E-04	5.0533E-04	5.4999E-04	6.0073E-04
a	46	47	48	49	50	51	52	53	54
f(a)	6.5868E-04	7.2523E-04	8.0200E-04	8.9105E-04	9.9502E-04	1.1172E-03	1.2616E-03	1.4335E-03	1.6399E-03
a	55	56	57	58	59	60	61	62	63
f(a)	1.8898E-04	2.1948E-	2.5713E-	3.0404E-	3.6319E-	4.3875E-	5.3673E-	6.6585E-	8.3965E-

		04	03	03	03	04	04	03	03
a	64								
f(a)	1.0776E-02								

For Laminate 2-Pure Glass									
Crack length a (mm)	19	20	21	22	23	24	25	26	27
f(a)	4.675E-05	4.947E-05	5.226E-05	5.518E-05	5.820E-05	6.137E-05	6.470E-05	6.821E-05	7.192E-05
a	28	29	30	31	32	33	34	35	36
f(a)	7.587E-05	8.008E-05	8.459E-05	8.94E-05	9.47E-05	1.00E-04	0.000107	0.000113	0.000121
a	37	38	39	40	41	42	43	44	45
f(a)	0.000129	0.000138	0.000148	0.000159	0.00017121	0.00018514	0.00020086	0.00021859	0.00023877
a	46	47	48	49	50	51	52	53	54
f(a)	0.0002618	0.00028822	0.00031868	0.00035396	0.00039507	0.0004433	0.00050017	0.00056773	0.00064867
a	55	56	57	58	59	60	61	62	63

f(a)	0.00074638	0.00086544	0.001012	0.0011945	0.0014242	0.0017174	0.002097	0.002598	0.003272
a	64								
f(a)	0.004196								

For Laminate 3-Hybrid (H1): G/AT/G/AT/G/AT/G									
Crack length, a (mm)	19	20	21	22	23	24	25	26	27
f(a)	6.175E-05	6.542E-05	6.919E-05	7.313E-05	7.72E-05	8.146E-05	8.593E-05	9.064E-05	9.562E-05
a	28	29	30	31	32	33	34	35	36
f(a)	0.0001009	0.0001066	0.0001126	0.000119	0.000126	0.000134	0.000142	0.000151	0.000161
a	37	38	39	40	41	42	43	44	45
f(a)	0.000172	0.000184	0.000197	0.000212	0.000228	0.000247	0.000268	0.000292	0.000319
a	46	47	48	49	50	51	52	53	54
f(a)	0.000349	0.000385	0.000425	0.000472	0.000527	0.000592	0.000668	0.000758	0.000867

a	55	56	57	58	59	60	61	62	63
f(a)	0.000998	0.001158	0.001355	0.0016	0.001908	0.002303	0.002814	0.003487	0.004394
a	64								
f(a)	0.005636								

For Laminate 4-Hybrid (H2): G/G/AT/AT/AT/G/G									
Crack length, a (mm)	19	20	21	22	23	24	25	26	27
f(a)	6.175E-05	6.542E-05	6.919E-05	7.313E-05	7.72E-05	8.146E-05	8.593E-05	9.064E-05	9.562E-05
a	28	29	30	31	32	33	34	35	36
f(a)	0.0001009	0.0001066	0.0001126	0.000119	0.000126	0.000134	0.000142	0.000151	0.000161
a	37	38	39	40	41	42	43	44	45
f(a)	0.000172	0.000184	0.000197	0.000212	0.000228	0.000247	0.000268	0.000292	0.000319
a	46	47	48	49	50	51	52	53	54

f(a)	0.000349	0.000385	0.000425	0.000472	0.000527	0.000592	0.000668	0.000758	0.000867
a	55	56	57	58	59	60	61	62	63
f(a)	0.000998	0.001158	0.001355	0.0016	0.001908	0.002303	0.002814	0.003487	0.004394
a	64								
f(a)	0.005636								